NUREG/CR-2030
BMI-2077
R2

Application of Battelle's Mechanistic Model to Lower Plenum Refill

Manuscript Completed: February 1981
Date Published: March 1981

Prepared by
A. Segev, R. P. Collier

Battelle Columbus Laboratories
505 King Avenue
Columbus, OH 43201

Prepared for
Division of Reactor Safety Research
Office of Nuclear Regulatory Research
U.S. Nuclear Regulatory Commission
Washington, D.C. 20555
NRC FIN A4048

ABSTRACT

A mechanistic model has been developed to describe the refill process of ECC during a postulated LOCA. The model analyzes a one-dimensional liquid film draining down a heated wall, in the presence of countercurrent steam flow. The effects of nonequilibrium void generation and steam condensation were investigated. These effects were incorporated into a momentum transfer correlation which was developed from air-water data in 1/15- and 2/15-scale models of a PWR, with standard and distorted geometries. This correlation is based on the Kutateladze parameter and indicates that the overall momentum transfer between the phases does not depend on scale for geometrically similar models. Theoretical predictions were compared with results from steady-steam flow tests in 1/15, 2/15- and 1/5-scale models with adiabatic walls, hot wall tests with steady and ramped steam flows, and with test L1-4 conducted in the LOFT facility. The comparisons exhibit fairly good agreement. When applied to a full scale PWR, the analysis predicts that ECC penetration would occur at a time shorter than the recommended licensing time delay, even when highly conservative assumptions are made.

TABLE OF CONTENTS

LIST OF FIGURES

LIST OF FIGURES
(Continued)

LIST OF FIGURES
(Continued)

LIST OF TABLES

I. INTRODUCTION

During a postulated loss-of-coolant accident (LOCA) due to a break in a cold leg of a large pressurized water reactor (PWR), emergency core cooling (ECC) water would be injected into the primary system piping to provide cooling for the reactor core. Depressurization during the blowdown phase of the LOCA would result in steam flow in the reverse direction down through the core and up the downcomer annulus. This upward steam flow in the annulus has the potential to retard or even prevent the penetration of the injected ECC fluid to the lower plenum (Figure 1).

Extensive experimental studies of the downcomer behavior have been conducted at Battelle-Columbus (BCL)[1] and at Creare[2] in PWR models of different scales. It was found that the penetration phenomenon is very chaotic in nature, involving complicated thermal and hydrodynamic effects. Thus, purely theoretical approaches often face numerous difficulties, and the use of empirical correlations is necessary.

Semi-empirical correlations have been constructed by several investigators using numerical "best fits" to test data[3,4,5,6]. These correlations include functional dependencies based on physical reasoning where possible. The best-estimated model developed by Creare describes the combined effects of steam upflow and hot wall steam on the liquid penetration behavior. This analysis was shown to be sensitive to the models chosen for interfacial exchange of momentum, and energy, and wall-to-fluid energy transfer. When this analysis was applied to steam flow transients at full scale with extreme assumptions for the adjustable parameters it was found that the calculated delivery time delay was unacceptably longer than the licensing delay time. The long delay time was predicted because the parameter which describes partition of wall heat between steam generation and liquid heating could not be bounded realistically.

To overcome this weakness an alternative method of calculating hot wall effects was developed by Segev and Collier[7] [8]. This mechanistic model was based on the simple flow pattern of a liquid film draining down a heated wall, assuming that this one-dimensional flow configuration represented the average chaotic phenomenon which occurs in the downcomer. Standard mass and energy conservation equations were coupled with an empirical flooding correlation which represents the net result of momentum

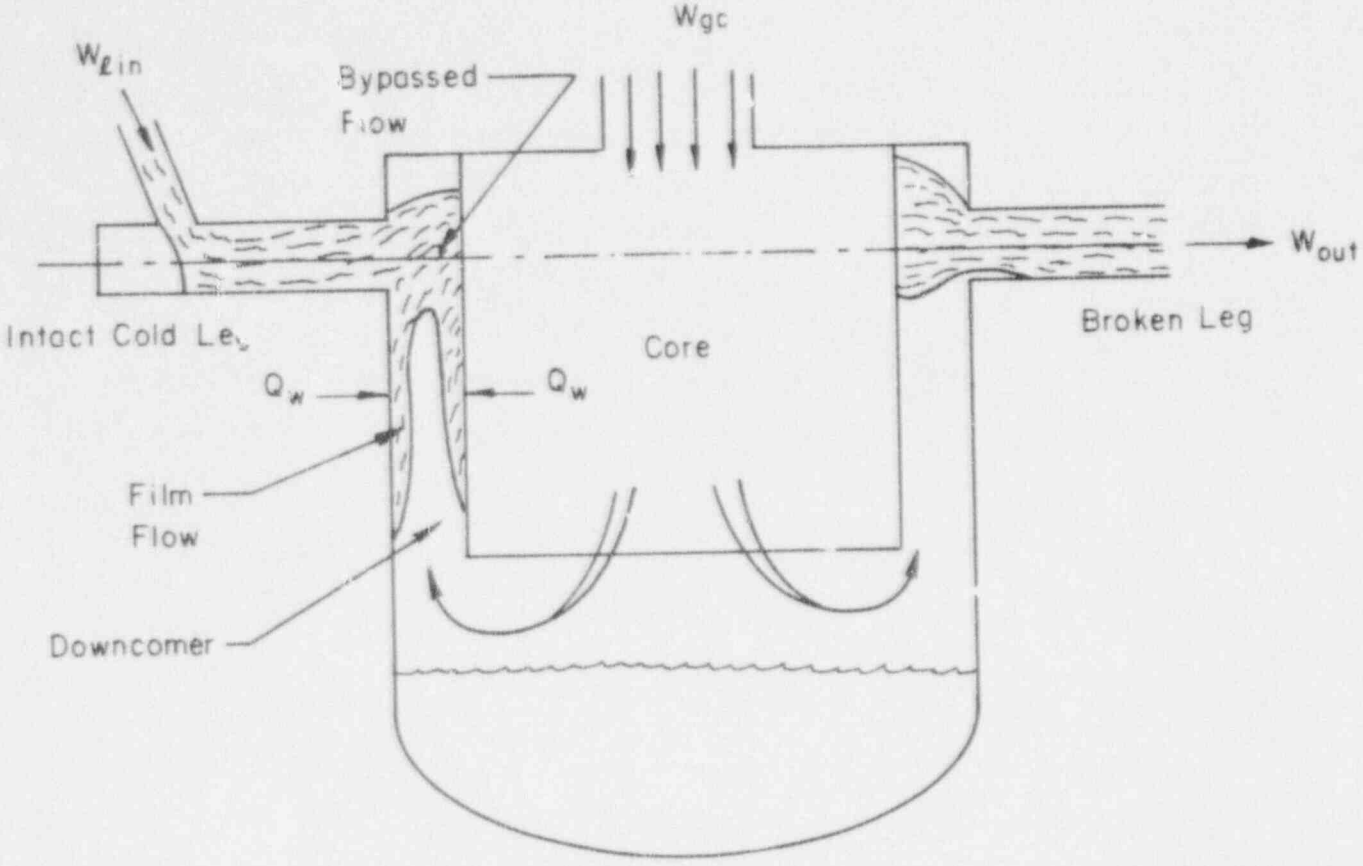

Geometry	1/15 BCL	2/15 BCL	1/5 Creare	LOFT	Full-Scale PWR
Gap Size, S	1.5	3.1	3.8	5.1	25.4
Downcomer length, L	41.0	82.0	137.2	425.6	533.4
Average Annulus Circumference, C_a	91.85	184.5	268.2	279.4	1285.2

Figure 1. Schematic Sketch of a Reactor Vessel (All units in cm)

exchange in the system. When this mechanistic model was applied to full scale, the calculated time delays were all shorter than the current licensing model, even when the most conservative assumptions were made in the analysis.

To substantiate these findings,additional data analysis has been conducted. This includes comparison with results from hot wall tests in 1/15-and 2/15-scale models and recent tests conducted in a 1/3-scale model. As a result, some modifications have been made in the mechanistic model. In this report, we will present the modified model and its application to the available data. We will also describe the results obtained from applying the model to full scale.

II. BATTELLE'S MECHANISTIC MODEL

Two exchange processes are involved during ECC penetration: momentum exchange and mass exchange. We will begin by discussing the complicated process of momentum exchange between the upflow steam and the downflow liquid film. It was shown in Reference 7 that the momentum exchange can be adequately described by a flooding correlation which represents the net result of this exchange. The flooding correlation may be considered as a limiting hydrodynamic relationship in which the upward gas flow rate controls the partitioning of the inlet liquid flow, $W_{\ell in}$, into a liquid flow which penetrates to the lower plenum as a film on the downcomer walls, $W_{\ell i}$, and bypassed liquid, $W_{\ell in} - W_{\ell i}$, which flows toward the outlet. (Figure 2.)

Momentum exchange effects may be isolated from the effects of mass exchange by conducting tests with steam and saturated water or with air and water. Experiments with both fluid combinations in the same test facility have shown that liquid penetration behavior is identical when described in terms of suitably nondimensionalized momentum fluxes. This suggests that air-water data can be used to understand the momentum exchange between steam and saturated water in countercurrent flow.

Experimental and theoretical studies in tubes or in annuli can provide insight into the momentum exchange phenomenon. However, in view of the strong dependence on geometry and flow configuration it is questionable whether the theoretical models or correlations developed in those geometries can be applied directly to the complicated flows in scaled models of PWR's. To minimize the consideration of these effects when analyzing momentum exchange in PWR-like geometries, air-water experiments have been conducted in 1/15- and 2/15-scale models of a PWR.

These tests were carried out for a range of air and water injection flow rates and water temperatures[9]. Typical test results are presented in Figure 3a using the Wallis parameter, which is defined as

$$J_x^* = [\rho_x j_x^2 / g C_a (\rho_\ell - \rho_g)]^{1/2} \quad , \qquad (1)$$

where j_x is the superficial velocity of phase x and C_a is the average annulus

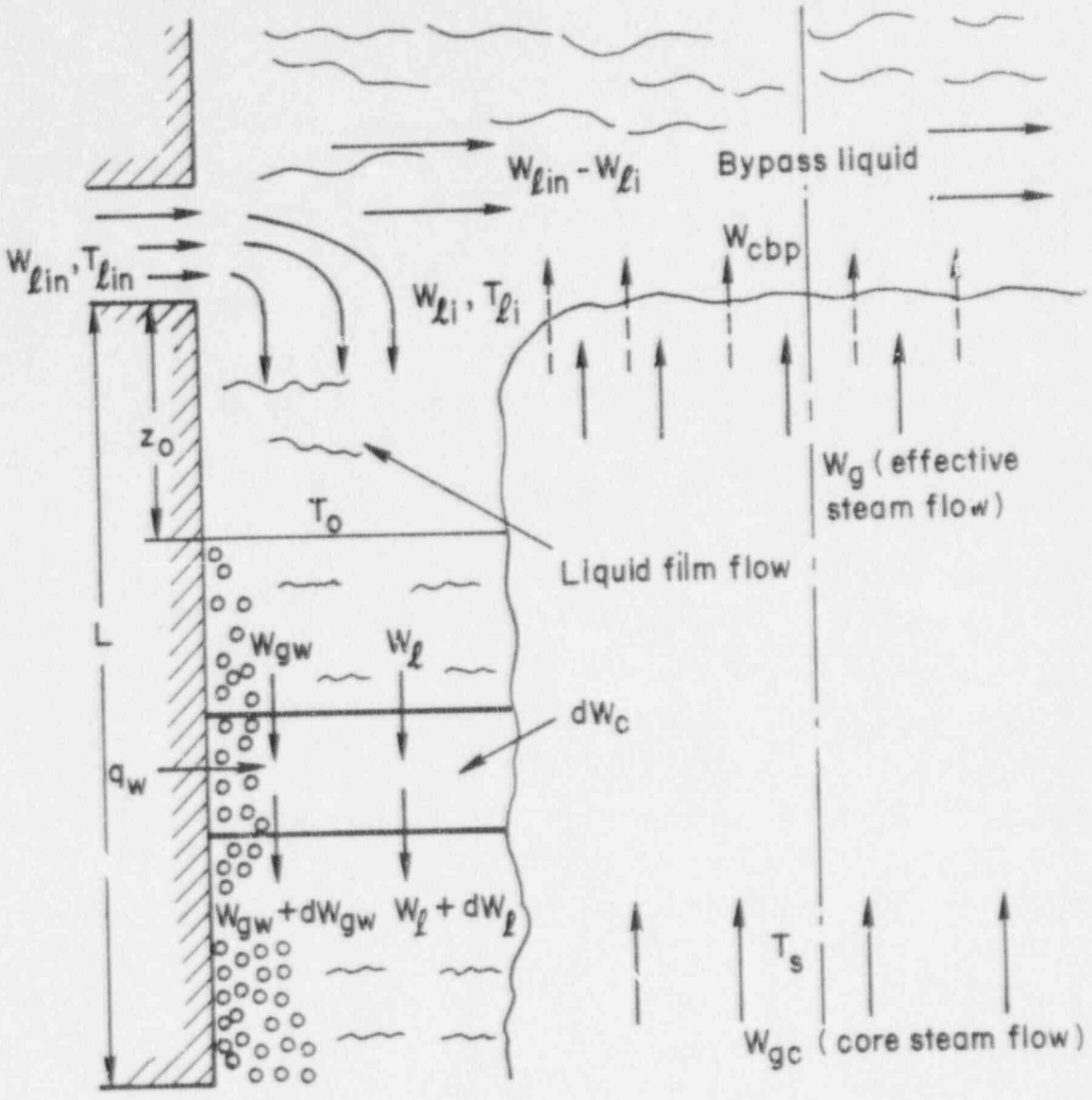

Figure 2. Schematic Sketch of a Falling Liquid Film In Countercurrent Flow

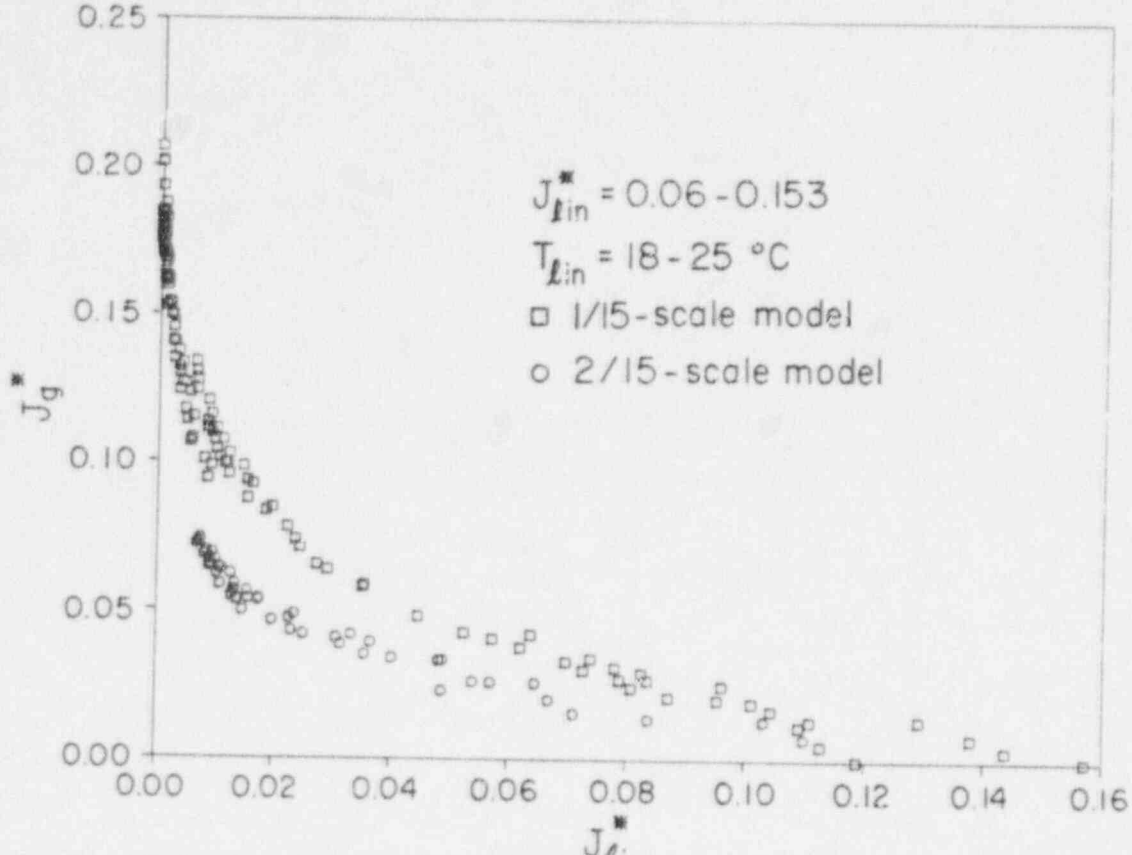

Figure 3a. Experimental Results with Air-Water Flows in 1/15- and 2/15-Scale Models (J^* Parameter)

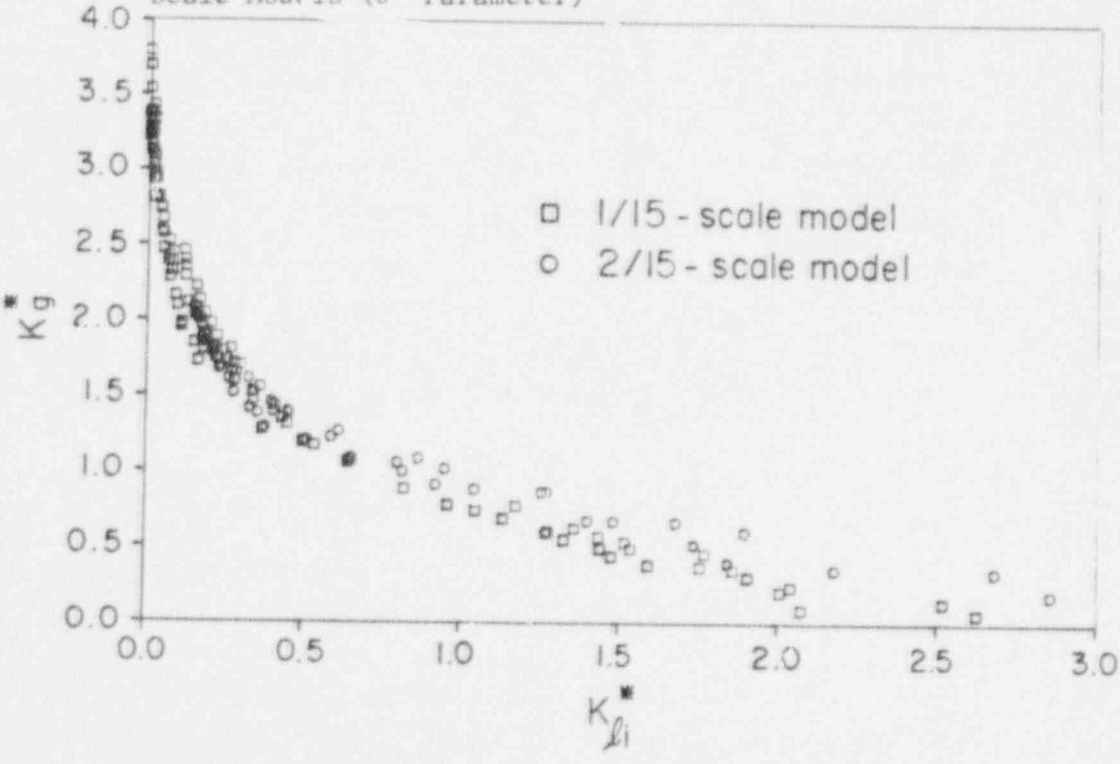

Figure 3b. Experimental Results with Air-Water Flows in 1/15- and 2/15-Scale Models (K^* Parameter)

circumference. It is clear that the data from the two different models do not overlay on J^* coordinates, but form two distinct curves. When compared to 2/15-scale data, the 1/15-scale data show increased penetration for a given dimensionless gas flux, J_g^*.

Figure 3b compares the same data using the Kutateladze number, which is defined as

$$K_x^* = (\rho_x j_x^2)^{1/2} / [g\sigma (\rho_\ell - \rho_g)]^{1/4} \quad , \qquad (2)$$

where σ is the gas-liquid surface tension. As shown, the data from both models converge much more closely than they did when compared with the J^* parameter. Thus, we conclude that a correlation based on the K^* parameter is more suitable for scaling air-water data in scaled models of a PWR. Utilizing the available air-water data from 1/15- and 2/15-scale models (including data from distorted 2/15-scale geometries) we have constructed a new interphase momentum transfer correlation in the form

$$K_g^{*\,1/2}(1 + K_{\ell i}^*) = (4C_a/L)^{1/4} \quad , \qquad (3)$$

Equation (3) indicates that for a fixed gas flux the liquid penetration depends only on the length-to-circumference aspect ratio, so it is independent of scale for geometrically similar models. This flooding correlation also indicates that the complete bypass point, $K_g^* = (4C_a/L)^{1/2}$, does not vary with scale for geometrically similar models and its value, $K_g^* \approx 3.0$, is close to the value 3.2 suggested as a criterion for complete bypass in tubes with large diameters[10].

Figure 4 compares the available air-water experimental data and the momentum exchange correlation of Equation (3); reasonably good agreement is shown. Note that the effects of liquid injection rate (as in the short core barrel tests) and liquid temperature (as in the extended core barrel tests) are not accounted for in this correlation. We have accepted these shortcomings for the sake of simplicity.

It is interesting that if one defines a parameter m as:

$$m = (K_g^* K_{\ell i}^*)^{1/2} \qquad (4)$$

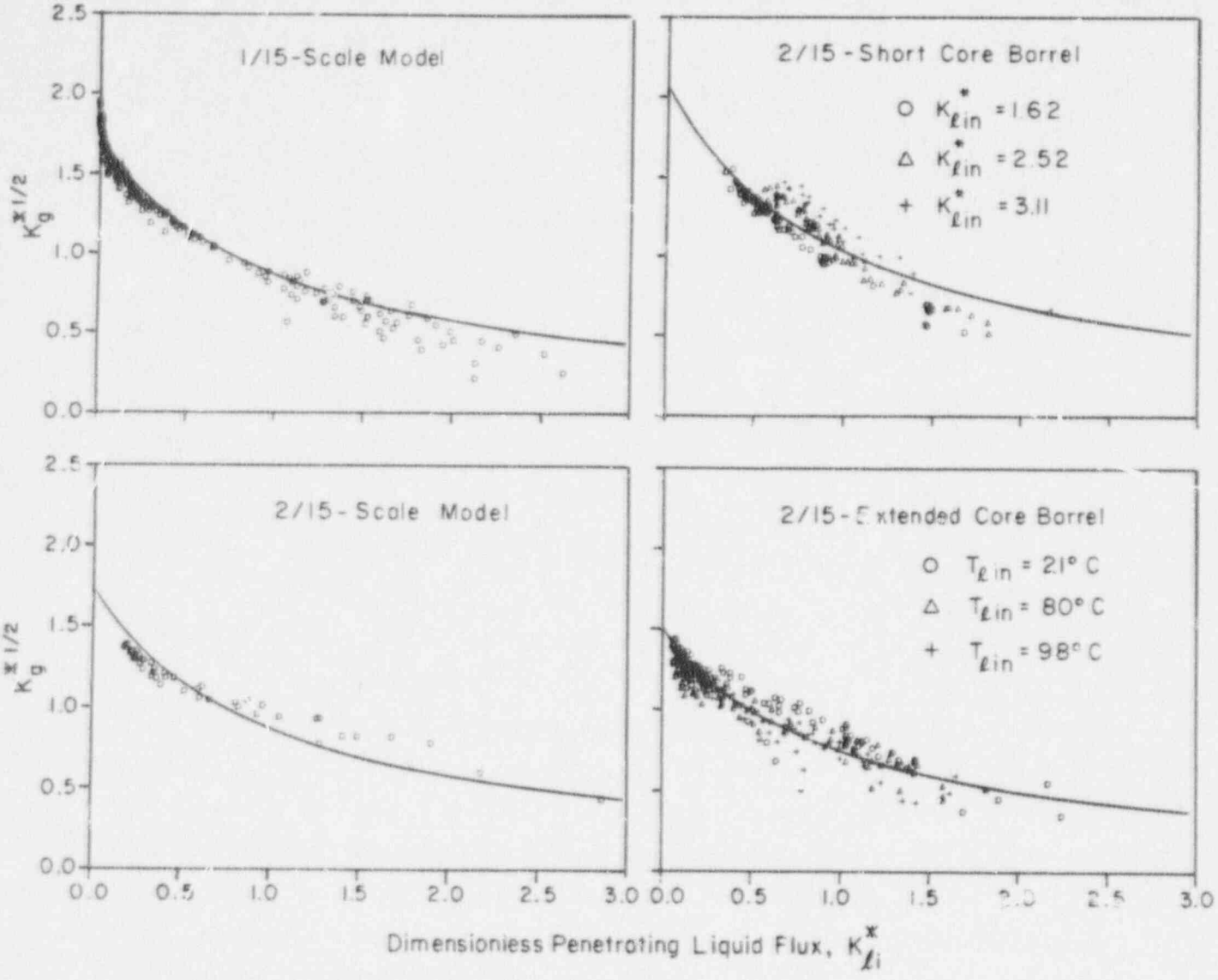

Figure 4. Comparison Between Air-Water Experimental Results and Momentum Exchange Correlation of Equation (3)

then the momentum exchange correlation of Equation (3) can be written as:

$$K_g^{*1/2} + mK_{\ell i}^{*1/2} = \left(\frac{4C_a}{L}\right)^{1/4} \qquad (5)$$

or:

$$J_g^{*1/2} + mJ_{\ell i}^{*1/2} = C \qquad (6)$$

where

$$C = \left\{\frac{4}{I}\left[\frac{\sigma}{g(\rho_\ell - \rho_g)}\right]^{1/2}\right\}^{1/4} \qquad (7)$$

Equation (6) can readily be identified as the Wallis flooding correlation[11] if the parameter m is assumed to be constant along the penetration curve. The parameter can be rewritten as:

$$m = \frac{K_{\ell i}^{*1/2}}{1 + K_{\ell i}^{*}} \left(\frac{4C_a}{L}\right)^{1/4} \qquad (8)$$

and is almost constant for $K_{\ell i}^{*} \geq 0.5$. Thus, the data in the high penetration region can be well represented by a linear relationship in the form of Equation (6). However, for $K_{\ell i}^{*} < 0.5$ (the high bypass region), m is strongly dependent on $K_{\ell i}^{*}$ and cannot be considered as a constant. Thus, the experimental data in this region will deviate from the straight line predicted by Wallis correlation. These conclusions are consistent with the experimental results in a 2/15-scale annuli with side injection[12].

Equation (4) suggests that any reduction in the effective steam flow rate, K_g^{*}, would result in an equivalent decrease in m. Thus, for steam-water flows, the value of m will decrease when the condensation potential increases (e.g. increase in liquid subcooling). This agrees with the findings of Creare[13] or Beckner et al[5].

The second exchange process which is important in ECC penetration is interphase mass transfer. The main components of the mass transfer are condensation of steam on the injected subcooled water and steam generation on the superheated walls.

The dimensionless net mass exchange along the penetrating liquid film, K^*_{tm}, is given by [8]:

$$K^*_{tm} = Q^* - f\lambda K^*_{\ell i} \tag{9}$$

where

$$Q^* = \frac{Q}{A[\rho_g{}^2 g\sigma(\rho_\ell - \rho_g)]^{1/4} h_{fg}} \tag{10}$$

$$\lambda = \frac{C_p(T_s - T_{\ell i})}{h_{fg}} \left(\frac{\rho_\ell}{\rho_g}\right)^{1/2} \tag{11}$$

$$f = \frac{T(L) - T_{\ell i}}{T_s - T_{\ell i}} \tag{12}$$

The parameter λ may be regarded as the condensation potential. The parameter f represents the effectiveness of energy transferred to the liquid from the hot walls and from condensation.

When applying the one-dimensional analysis to ECC penetration in PWR scaled models, condensation is not limited only to condensation along the liquid film. Additional condensation occurs on the liquid which is being bypassed. This condensation component is denoted by the nondimensional parameter K^*_{cbp} and will be evaluated below.

The effects of mass transfer on the momentum exchange may be described by modifying the momentum exchange correlation of Equation (3). This can be done by considering K^*_g to be the effective gas flow rate for momentum exchange. In other words, K^*_g in Equation (3) is the net steam flow rate at the liquid entrance region. It consists of externally supplied steam (K^*_{gc}) and net mass exchange along the film (K^*_{tm}) and on the bypassed liquid:

$$K^*_g = K^*_{gc} + K^*_{tm} - K^*_{cbp} \tag{13}$$

Substituting Equations (9) and (12) into Equation (3) we obtain

$$\left(K^*_{gc} - f\lambda K^*_{\ell i} - K^*_{cbp} + Q^*\right)^{1/2}\left(1 + K^*_{\ell i}\right) = \left(\frac{4C_a}{L}\right)^{1/4} \qquad (14)$$

Let us examine now the special case in which the walls are adiabatic. In this case $Q^* = 0$ and f represents the condensation efficiency of steam on the countercurrent liquid film. From a separate effect study [14] it was found that f is given by

$$f = 1 - \exp\left(-1.34 \times 10^{-4} \frac{Re_g^{0.30}}{Re_\ell^{0.27}} \frac{L}{t}\right) \qquad (15)$$

where t is the film thickness and Re_x is the Reynolds number of phase x, defined as

$$Re_x = \frac{W_x}{\mu_x C_a} \qquad (16)$$

The best agreement between the theoretical predictions and the experimental results from scaled models was obtained when the film thickness was assumed to be 3.5×10^{-4} L.

For the case in which all injected liquid is bypassed $\left(K^*_{\ell i} = 0\right)$, Equation (14) can be written as

$$K^*_{gb} = \left(\frac{4C_a}{L}\right)^{1/2} + K^*_{cbp} \qquad (17)$$

where K^*_{gb} is the core steam flux which causes complete bypass. Obviously, the only mass exchange in the system at the complete bypass point occurs on the liquid being bypassed, which is essentially a turbulent liquid ring being held up in the downcomer. Thus, K^*_{cbp} can be evaluated if the complete bypass point is determined.

By studying the trends of the available complete bypass point data we found that condensation on the bypassed liquid can be described by:

$$K^*_{cbp} = f_1 \left\{ \lambda \left(K^*_{\ell in} - K^*_{\ell i} \right) \right\}^{1/2} D^{*n} \qquad (18)$$

where D^* is the Bond number,

$$D^* = C_a \left[\frac{g(\rho_\ell - \rho_g)}{\sigma} \right]^{1/2} \qquad (19)$$

and n is a constant, the value of which depends on scale.

The parameter f_1, may be regarded as the efficiency of steam condensation on the bypassed liquid, in an analogy to the steam condensation efficiency on the liquid film, described previously. Using the same analogy for the functional form, f_1 is correlated by

$$f_1 = 1 - \exp \left[-4.5 \times 10^{-3} \frac{\overline{Re}_g^{0.58}}{\overline{Re}_\ell^{0.26}} \left(\frac{C_a}{s} \right)^{0.32} \right] \qquad (20)$$

where the vapor and liquid Reynolds number are defined as

$$\overline{Re}_g = \frac{W_{gc} + W_{tm}}{\mu_g C_a} \qquad (21)$$

$$\overline{Re}_\ell = \frac{W_{\ell in} - W_{\ell i}}{\mu_\ell C_a} \qquad (22)$$

The values for f_1 used in evaluating the constants of Equation (20) were determined by solving Equation (14) for K^*_{cbp} and then Equation (18) for f_1, utilizing the available steam-water data.

To assess the correlation for K^*_{cbp}, the complete bypass point was calculated and compared to experimental data obtained from 1/15- and 2/15-scale models. Satisfactory agreement was obtained[8]. Equations (17) and (18) show that the complete bypass point increases with scale for given values of λ and $K^*_{\ell in}$. Also. K^*_{gb} increases with λ for a given scale, and its

sensitivity to changes in λ becomes more pronounced as scale increases. Thus, we may expect that penetration curves at larger scales will be more sensitive to condensation than in smaller scales. This is particularly true for high liquid temperatures (low subcoolings). In this case the relative changes in subcooling, and consequently, the relative changes in λ, are very significant. As an example, a subcooling of 3 C in a 1/5-scale model may result in an ~ 30 percent increase of K^*_{gb} from its value at saturation. This is shown later when 1/5-scale model data are presented.

For the case in which saturated water ($\lambda = 0$) is injected into the annulus, Equation (14) indicates that the effect of liquid injection flux diminishes and that the penetration curve would coincide with that of an air-water system. Practically speaking, however, it is extremely difficult to carry out countercurrent flooding experiments with saturated water at predetermined conditions. Any small peturbation in temperature or system pressure will result in flashing or condensation. As discussed before, even a slight deviation from the saturation conditions can lead to a significant amount of condensation, an effect which increases with scale.

Substitution of Equation (18) into Equation (14) yields the final form for the penetration curve equation:

$$\left\{K^*_{gc} - f\lambda K^*_{\ell i} - f_1\left[\lambda(K^*_{\ell in} - K^*_{\ell i})\right]^{1/2} D^{*n} + Q^*\right\}^{1/2} (1 + K^*_{\ell i}) = (4C_a/L)^{1/4} \qquad (23)$$

The steady steam flux necessary to bypass a given amount of liquid can be calculated from this equation. This was done in Reference 8 and the results obtained were in satisfactory agreement with the experimental data.

The pertinent dependent parameter to be predicted is the penetrating liquid flux, $K^*_{\ell p}$, which is approximately related to $K^*_{\ell i}$ by [7]:

$$K^*_{\ell p} = K^*_{\ell i} \exp\left(\frac{C_p \Delta T_s f}{h_{fg}}\right) \qquad (24)$$

As can be readily shown, Equation (23) is a sixth order polynominal equation for $K^*_{\ell i}$. Previous attempts to solve this equation resulted in difficulty, as the solution is very sensitive to changes in the coefficients which occur during the iteration process. An alternative method has been used here. Equation (23) was solved explicitly for K^*_{gc} as $K^*_{\ell i}$ varied from zero to $K^*_{\ell in}$. The vector of $K^*_{\ell i}$ values were then interpolated to obtain a value of $K^*_{\ell i}$ which corresponded to a given experimental value of K^*_{gc}. Finally, the liquid penetration flux was calculated from Equation (24).

Figures 5 and 6 compare theoretical predictions of penetrating liquid fluxes with experimental data obtained in the 1/15- and 2/15-scale models, respectively. We used 0.20 as the value for n in Equation (23) for the 1/15-scale model, and 0.25 for the 2/15-scale model. As shown, the agreement is relatively good for a wide range of flow conditions (pressures from 0.14 MPa to 0.55 MPa and injected liquid fluxes from $K^*_{\ell in}$ = 1.18 to 5.00). It was concluded that liquid penetration rate depends strongly on core steam flux (K^*_{gc}) and liquid subcooling, and to a lesser extent on lower plenum pressure and injected liquid flux. Subcooling and pressure effects are accounted for via the condensation potential parameter (λ) and the dimensionless steam flux. For a specific K^*_{gc}, liquid penetration increases when λ increases, i.e., when pressure and/or subcooling increased. Injected liquid flux affects the rate of condensation on the liquid bypassed, as is evident from Equation (18). An increase in $K^*_{\ell in}$ results in an increase in condensation and therefore an increase of liquid penetration.

Recent tests have been conducted by Creare in a 1/5-scale model[15]. The available data may be used to assess the predictive capability of the mechanistic model, which is based partially on correlation of air-water data and steam-water data in 1/15- and 2/15-scale models. Figure 7 shows two penetration curves calculated from Equation (23) for given test conditions in the 1/5-scale model. Assuming a linear dependence of n on scale, the value for n used in our calculation was 0.30. Also shown in Figure 7 are experimental test results for $K^*_{\ell in}$ = 3.70 and P = 0.21 MPa. Two different liquid temperatures were used: $\sim$ 100 C and $\sim$ 62 C, which correspond to $\sim$ 3 C and $\sim$ 41 C subcoolings, respectively. As shown, the agreement is quite good, indicating that condensation dependence on scale is reasonably described by Equation (23). The data also suggest that the scaling of momentum exchange

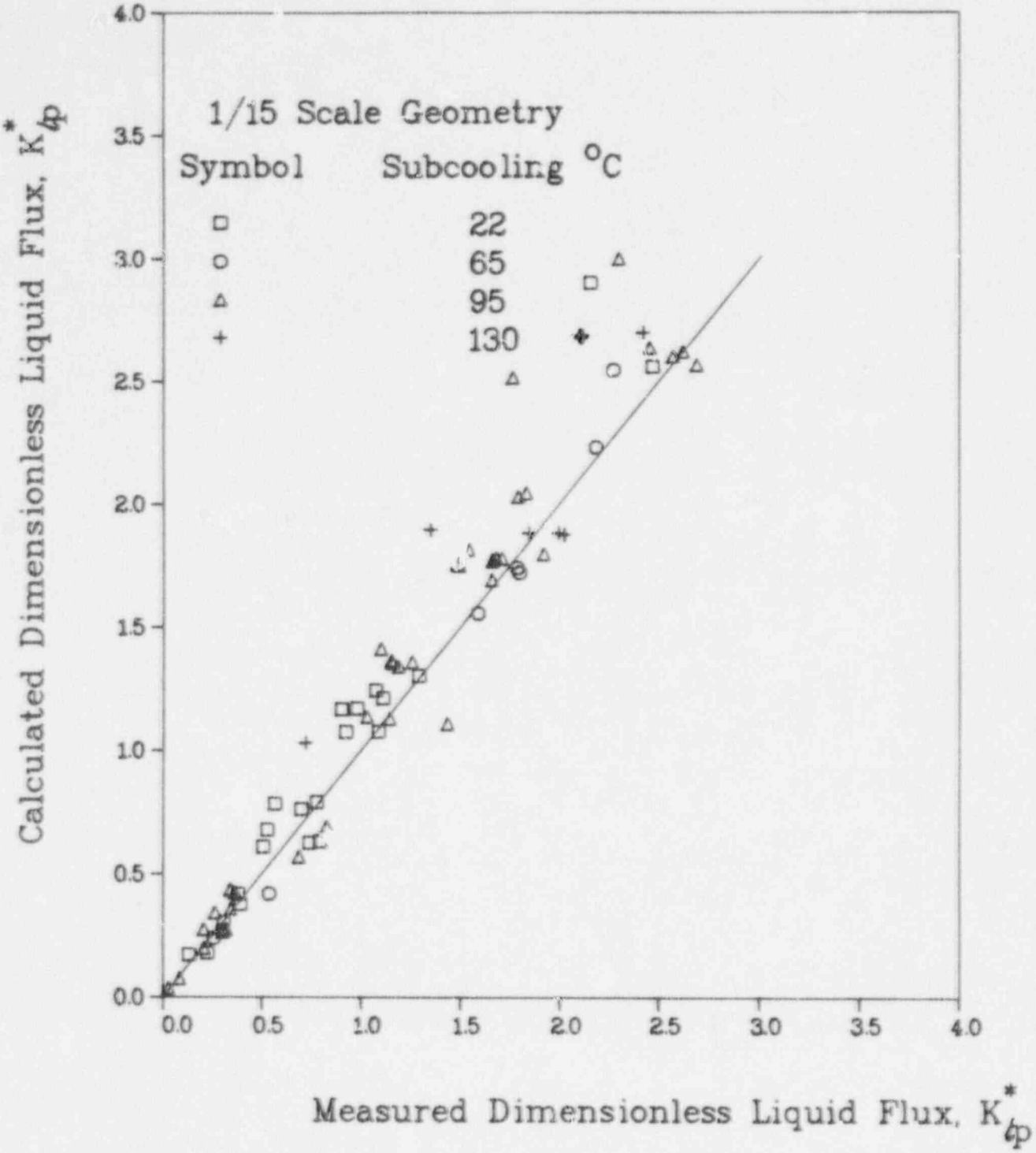

Figure 5. Comparison Between Calculated and Measured $K^*_{\ell p}$ for Battelle's 1/15-Scale Model

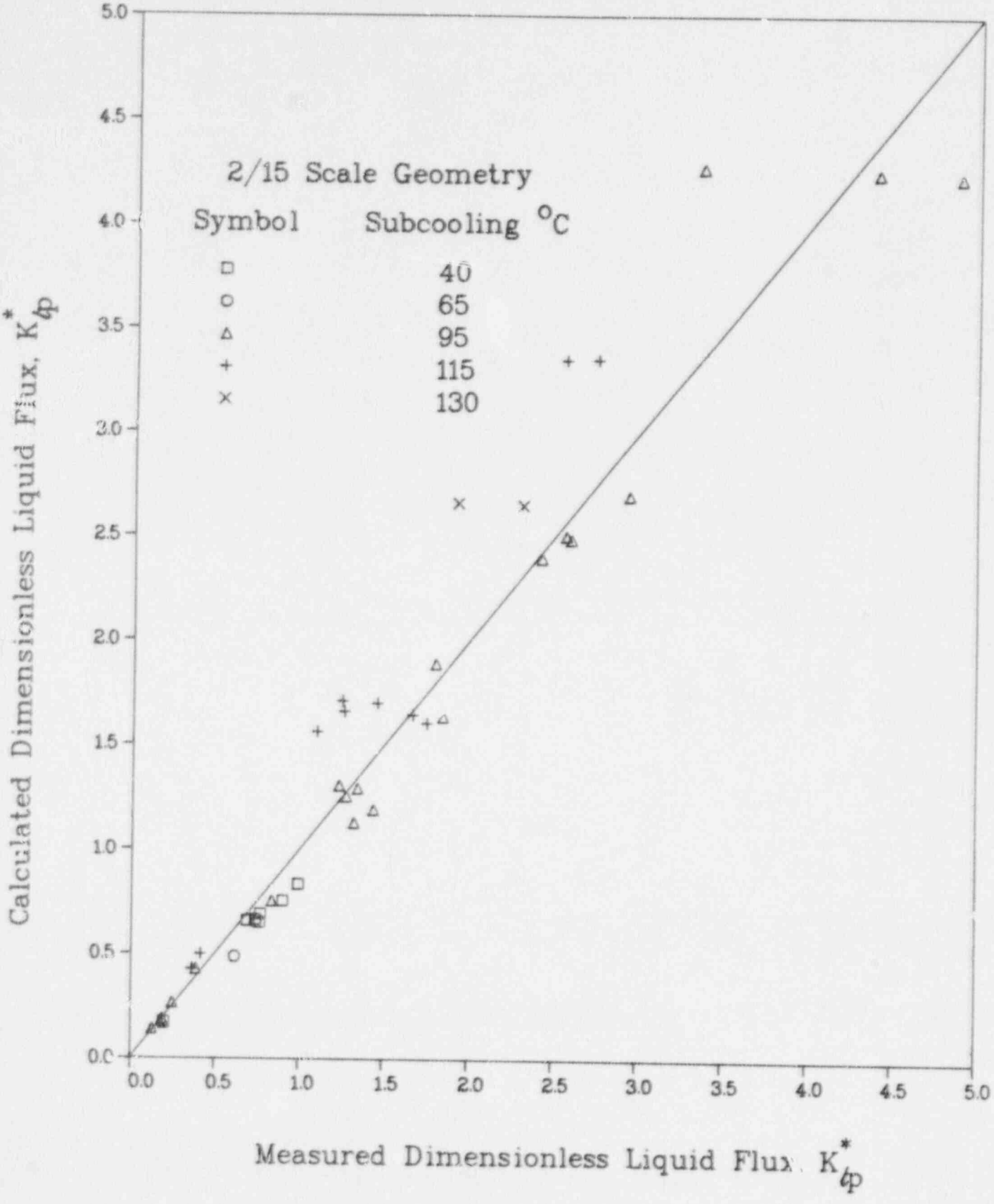

Figure 6. Comparison Between Calculated and Measured $K^*_{\ell p}$ for Battelle's 2/15-Scale Model

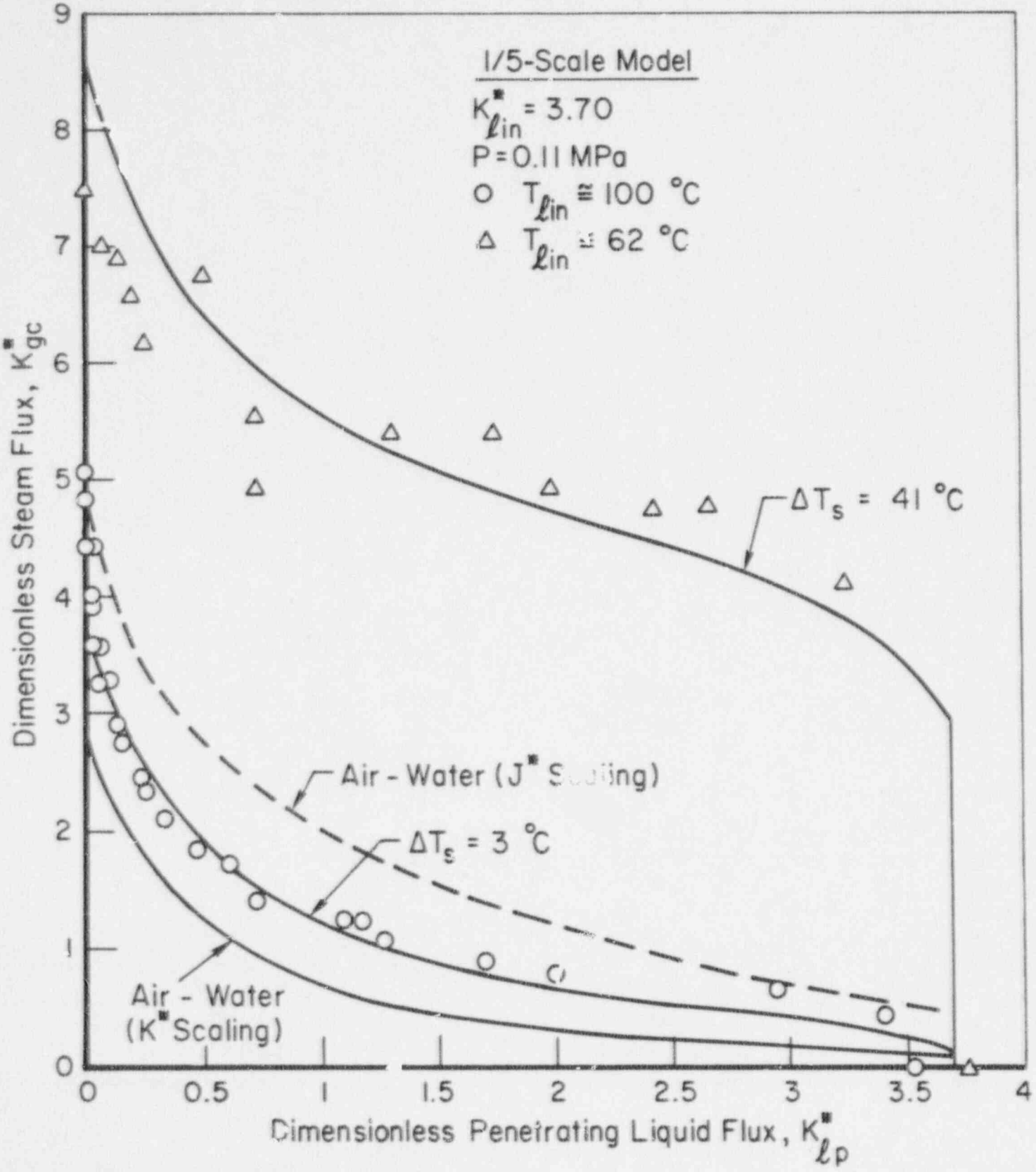

Figure 7. Prediction of Penetration Curves in 1/5-Scale Model

(air-water flooding) by a J^* parameter is not suitable for flows in PWR scaled models. This is evident from the low subcooling data which lie well below the J^* correlation suggested by Creare[13] for the scaling of air-water or steam-saturated water data:

$$J_g^{*1/2} + 0.8\, J_{\ell i}^{*1/2} = 0.4 \qquad (25)$$

On the other hand, the calculated low subcooling curve agrees quite well with the experimental data. This indicates that the scale dependence of momentum exchange is consistent with a K^* correlation such as Equation (3).

III. HOT WALL TESTS

The mechanistic model may be applied to tests where the vessel and the core barrel walls are initially superheated. The downflow of liquid in thi case is limited by the countercurrent upflow of vapor generated on the heated walls in addition to that from the core region. For tests in which the core steam flow is steady, a relatively simple closed-form expression can be derived for the liquid penetration time delay[8]. Even though this expression can be used in the evaluation of our model it is restricted to steady core steam flows. A different method is required to describe transient core steam flows. Also, by considering only the penetration delay times we ignore the initial transient penetration period, which may be significant in the theoretical description of the filling process. Therefore, an alternative procedure is required which will apply to both cases (steady and ramped steam flow) and will describe the complete lower plenum process.

The approach utilizied here is a numerical one, where the position of the liquid front in the downcomer is determined at any given time. For each time step, Δt, the value of $K^{*}_{\ell i}$ (t) is determined from the effective momentum correlation of Equation (23). For the hot wall tests we assume that f_1 is unaffected by the hot walls and that it represents only the steam condensation efficiency on the bypassed liquid. We also assume that the condensation heat transfer to the liquid film is negligible compared to the wall heat transfer. Thus, the parameter f represents the effectiveness of energy convection in the film, given by[8]

$$f = \left[1 - \exp\left(-\frac{L - z_o}{\Delta \ell}\right)\right] \frac{T_s - T_o}{T_\ell - T_{\ell i}} \qquad (26)$$

where $\Delta \ell$ is the significant boiling length and z_o is the point of net vapor generation, given by

$$z_o = \frac{W_{\ell i} C_p (T_o - T_{\ell i})}{P_h q_w} \quad . \qquad (27)$$

The liquid temperature at z_o is determined from the correlation developed by Saha & Zuber [16].

The dimensionless heat flux Q^* is described by Equation (10) where Q is given by

$$Q = P_h \int_{z_o}^{z} q_w dz \quad , \tag{28}$$

Assuming the heat flux, q_w, to be conduction limited, we get:

$$q_w = \frac{k_w(T_w - T_s)}{[\pi\alpha_w(t - t(z))]^{1/2}} \tag{29}$$

where $t - t(z)$ is the time period that any wetted point on the wall has been in contact with the liquid film.

After $K^*_{\ell i}(t)$ is evaluated we can determine the film velocity and the distance the film travels in the downcomer during the specified Δt, by assuming that the liquid film thickness is given by Nusselt equation. Subsequently, $z_o(t)$ and $Q^*(t)$ are determined and substituted back into Equation (23) to calculate $K^*_{\ell i}(t + \Delta t)$. This procedure repeats until the liquid front reaches the end of the core barrel and penetration is assumed to commence.

Figures 8 - 13 show a comparison between the calculated and experimental filling traces for a number of tests conducted in the 2/15-scale model [17]. Also shown are the experimental pressures in the lower plenum (P_v). The arrows in these figures indicate the time of liquid injection.

As may be noticed, the pressure traces describe quite well the resultant vapor generation during the tests. Upon the injection of liquid, vapor is generated at the hot walls of the downcomer, resulting in a pressure increase. The magnitude of this pressure increase depends mainly on inlet liquid and steam flow rates, inlet liquid temperature, and initial wall temperature. The maximum pressure in the lower plenum may reach a value twice as large as the pressure in the containment. For a given set of test conditions, an increase in wall temperature results in an increase of lower plenum pressure, suggesting that a larger amount of steam was

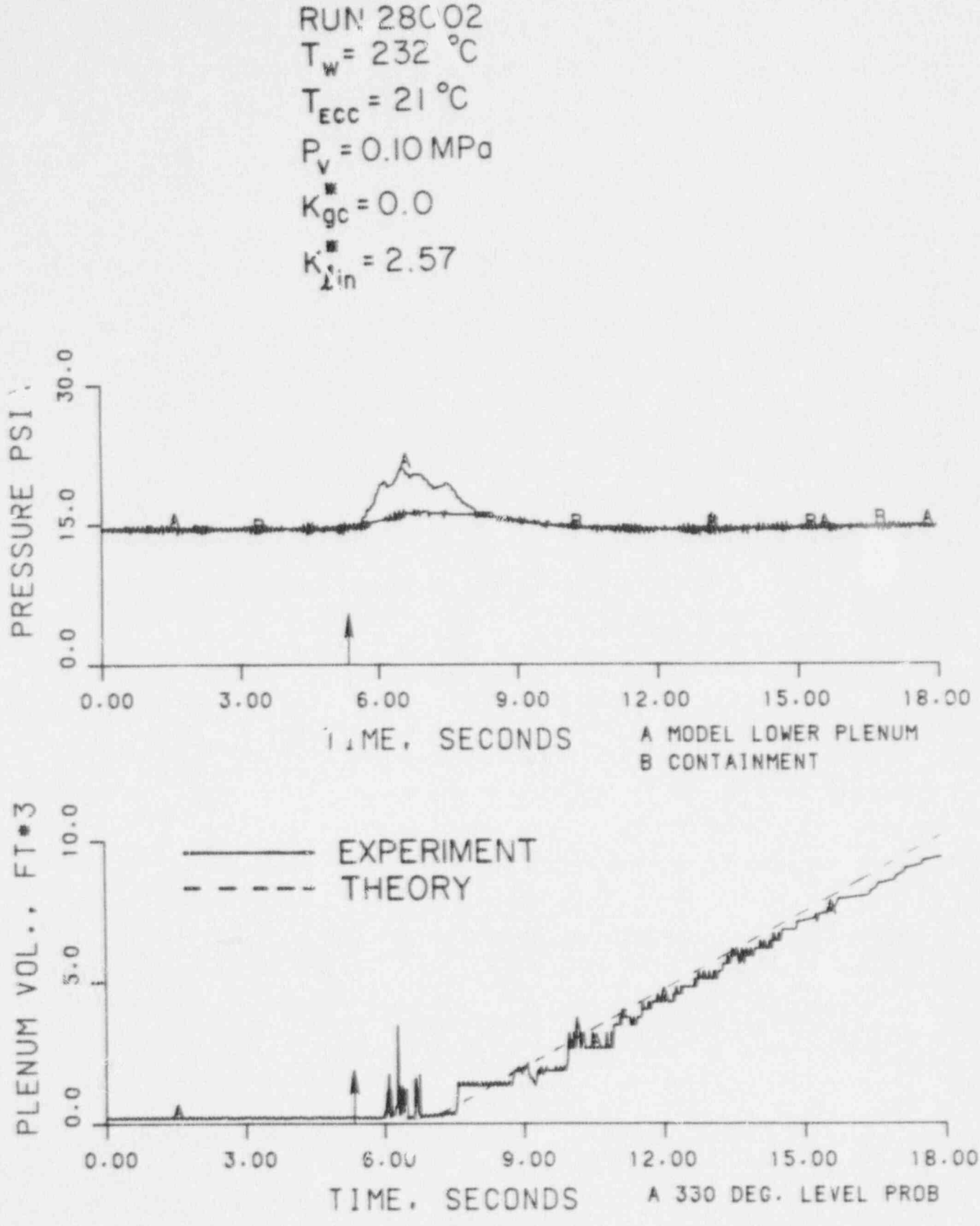

Figure 8. Theoretical and Experimental Results of Test 28002

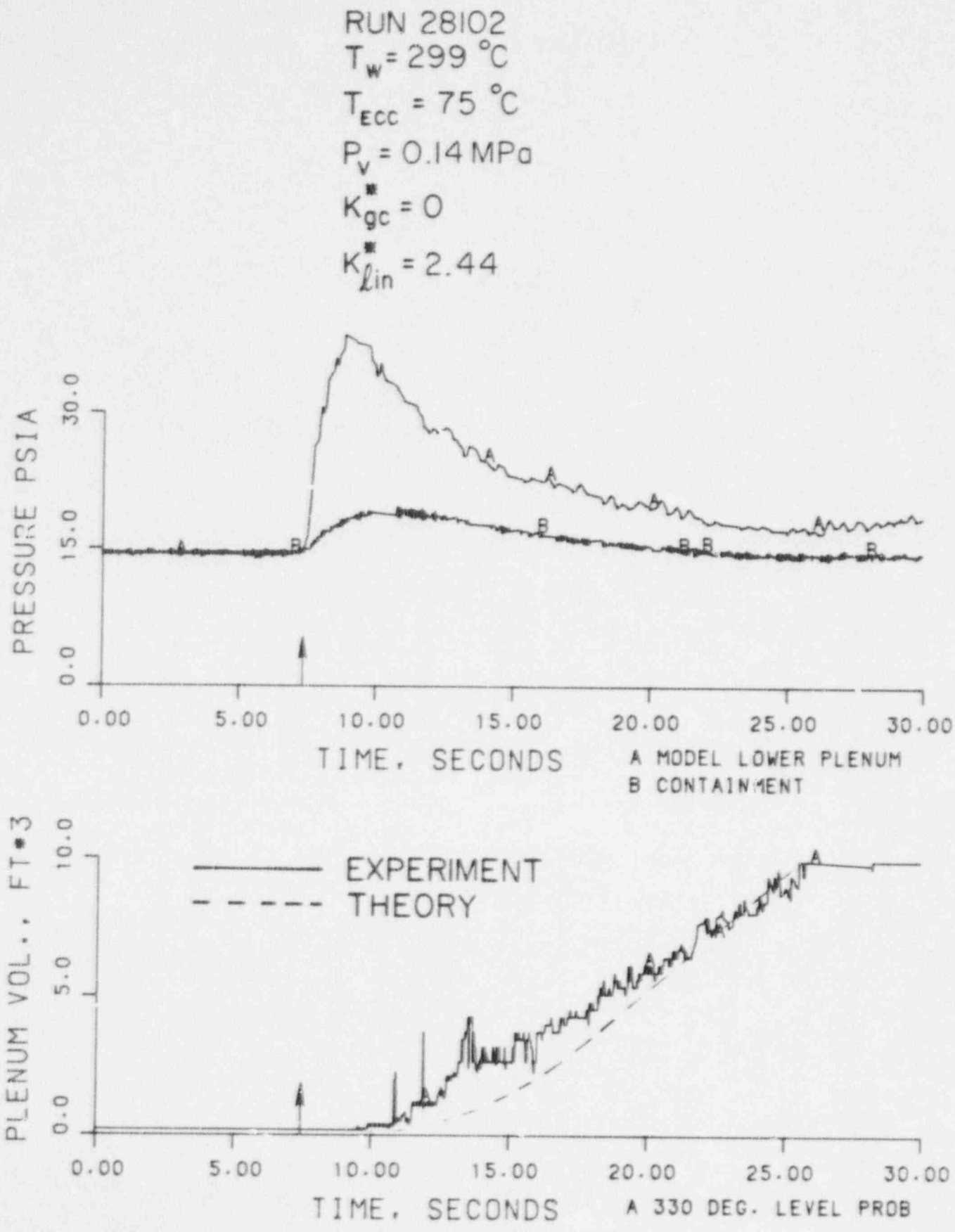

Figure 9. Theoretical and Experimental Results of Test 28102

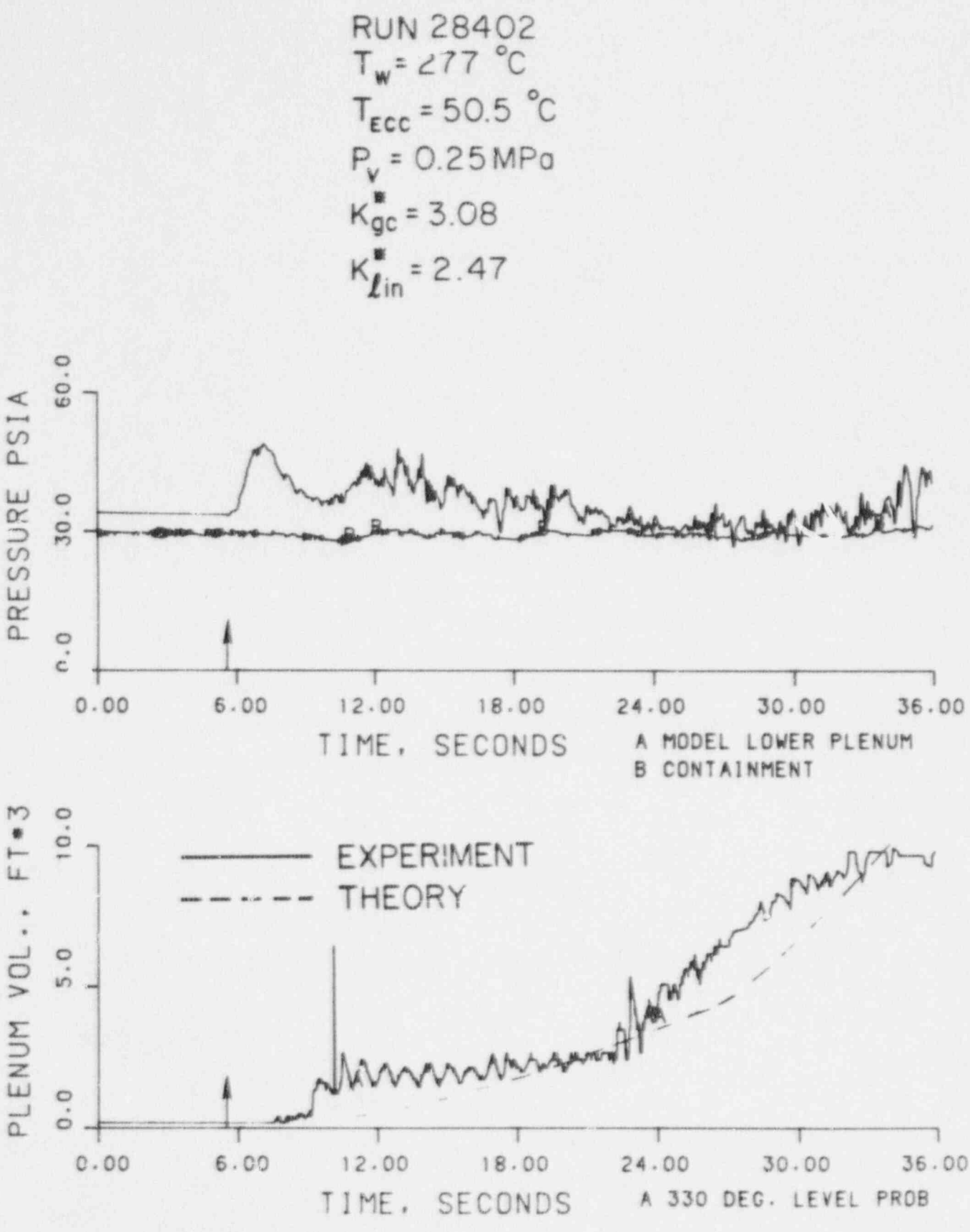

Figure 10. Theoretical and Experimental Results of Test 28402

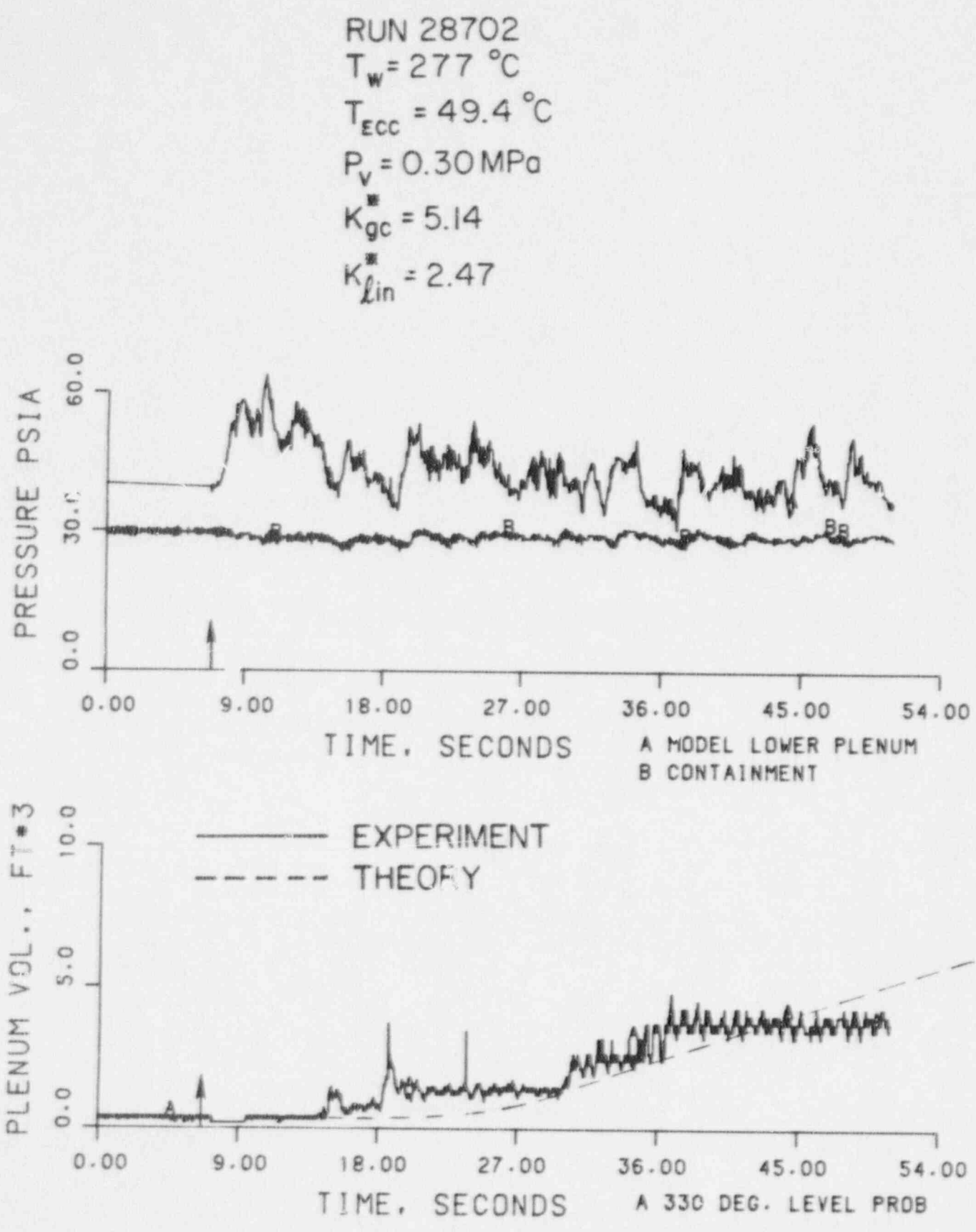

Figure 11. Theoretical and Experimental Results of Test 28702

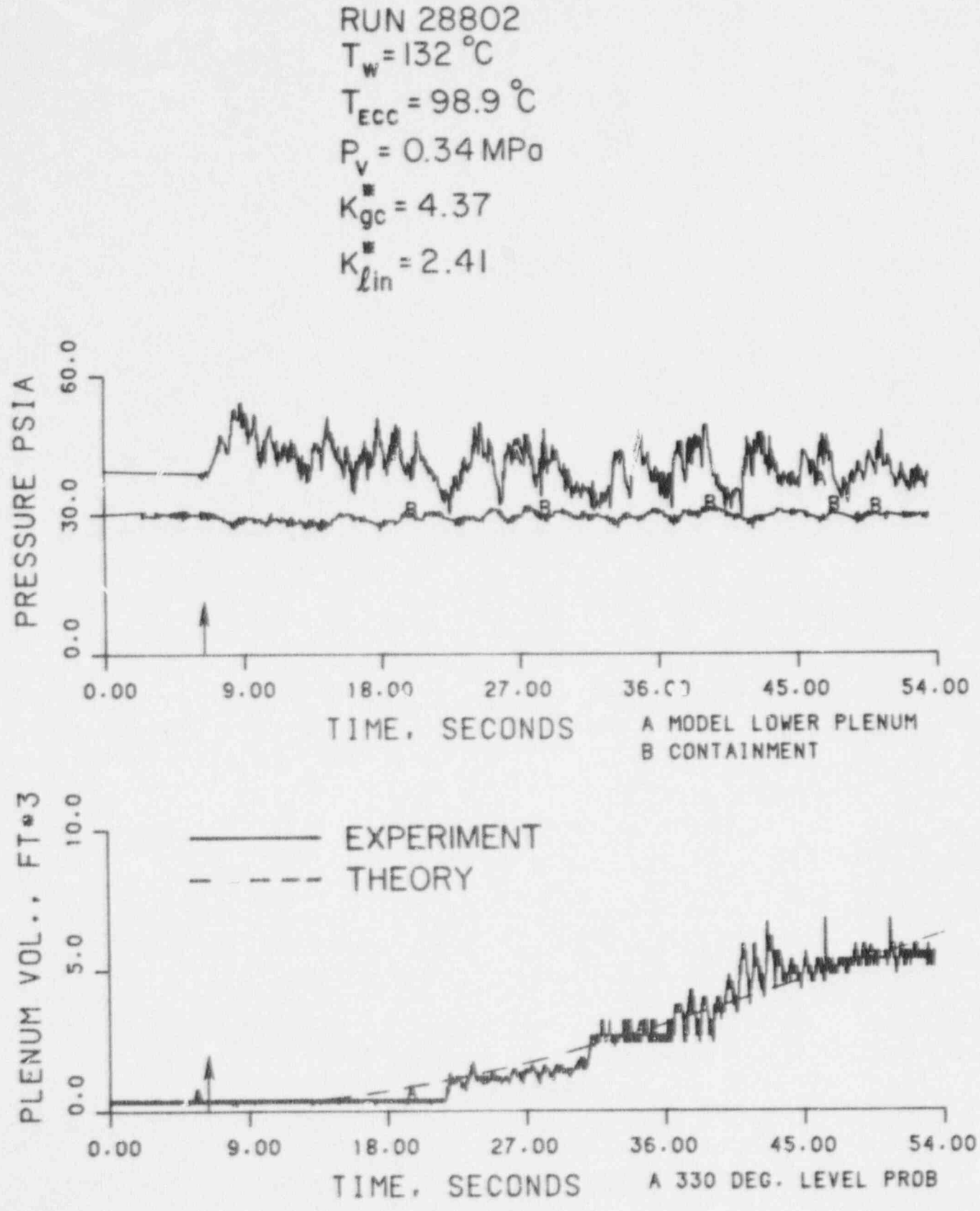

Figure 12. Theoretical and Experimental Results of Test 28802

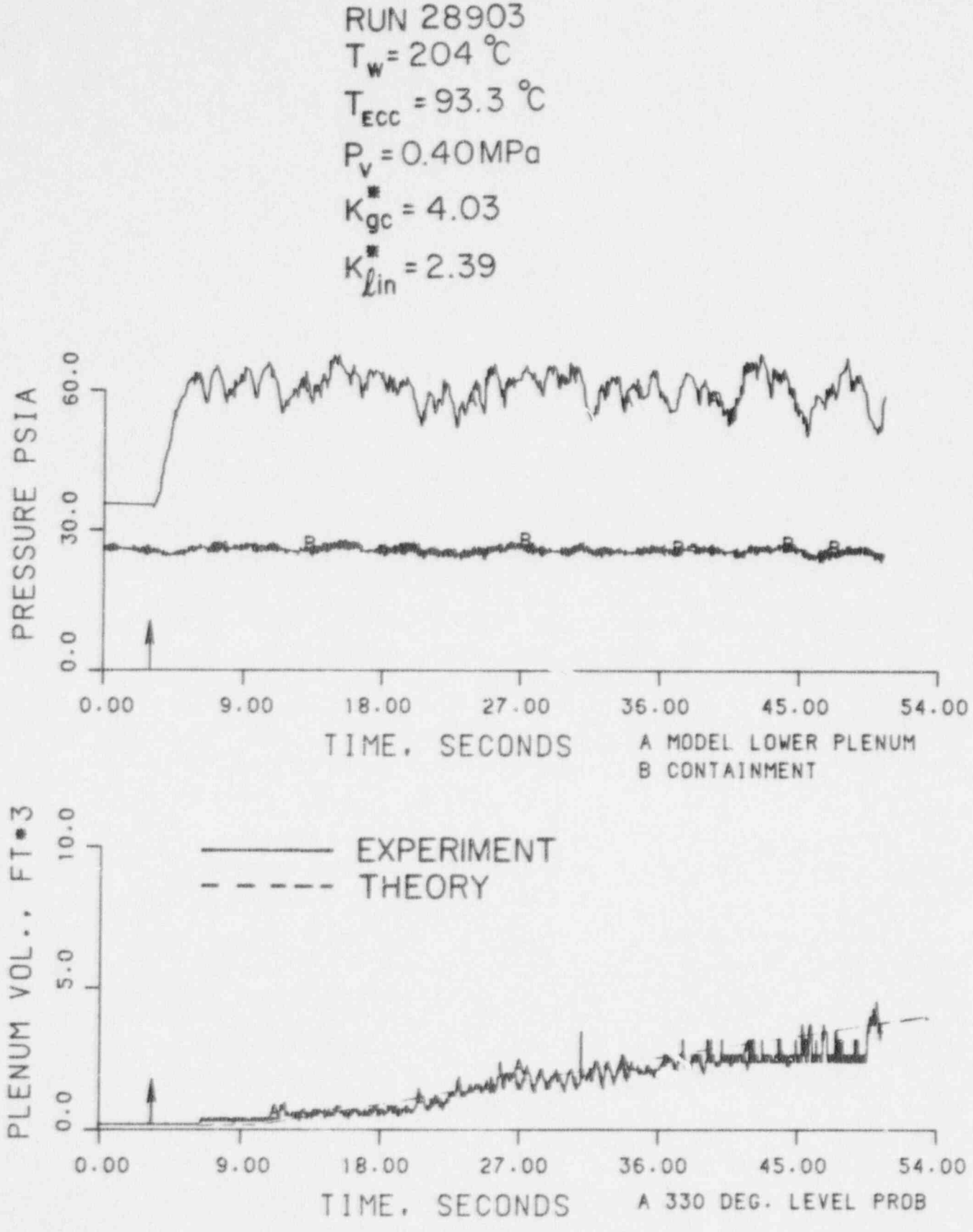

Figure 13. Theoretical and Experimental Results of Test 28903

generated. This is similar to the results obtained in vertical tube experiments[18]. However, even though more vapor is generated as wall temperature increases, no significant increase in time delay is observed. The explanation for that may be related to the competing effect of pressure on the penetration behavior. This point will be discussed later. After the pressure reaches its peak then decreases gradually to near ambient pressure (in cases when cold liquid is injected), or decreases slightly in an oscillatory manner (in cases when hot liquid is injected).

A typical plenum filling curve is characterized by a time delay before filling is observed. During this time delay the liquid front moves in the downcomer and vapor is generated at the hot walls. As the film reaches the end of the downcomer the lower plenum begins to fill at a low rate, which is transient and controlled by the wall vapor generation. When the vapor generation decreases significantly (due to decrease in wall heat flux and/or an increase in z_o) a shift in the penetration rate is noticed. The rate increases and becomes steady, controlled only by the core steam flow.

As shown in Figures 8 - 13 the calculated penetration delay time coincides in most tests to the time at which liquid first reaches the lower plenum and the calculated penetration rates are also in satisfactory agreement with the experiments.

The tests shown above were conducted with a scaled broken leg. To further investigate the effects of pressure build-up in the vessel, tests were conducted with an enlarged broken leg[19], resulting in a reduced pressure increase in the lower plenum. As shown in Figures 14 - 19 the mechanistic model accounts quite well for the changes in pressure and the agreement with the experiments is fairly good.

The mechanistic model was used to analyze cold plenum tests conducted by Creare[20] in their 1/15-scale model. In these tests, the lower plenum was cooled by subcooled water during the heat up of the annulus walls, resulting in a subcooled lower plenum. In this way, the effect of downcomer wall heat flux is isolated from possible effects of lower plenum heat flux. Figures 20-22 show the experimental results and the theoretical filling curves predicted by Creare's best estimate analysis and by our mechanistic model. In these figures the wall temperature is maintained at 177 C and

RUN 30202
T_w = 243 °C
T_{ECC} = 77.8 °C
P_v = 0.11MPa
K^*_{gc} = 0.0
$K^*_{\ell in}$ = 2.57

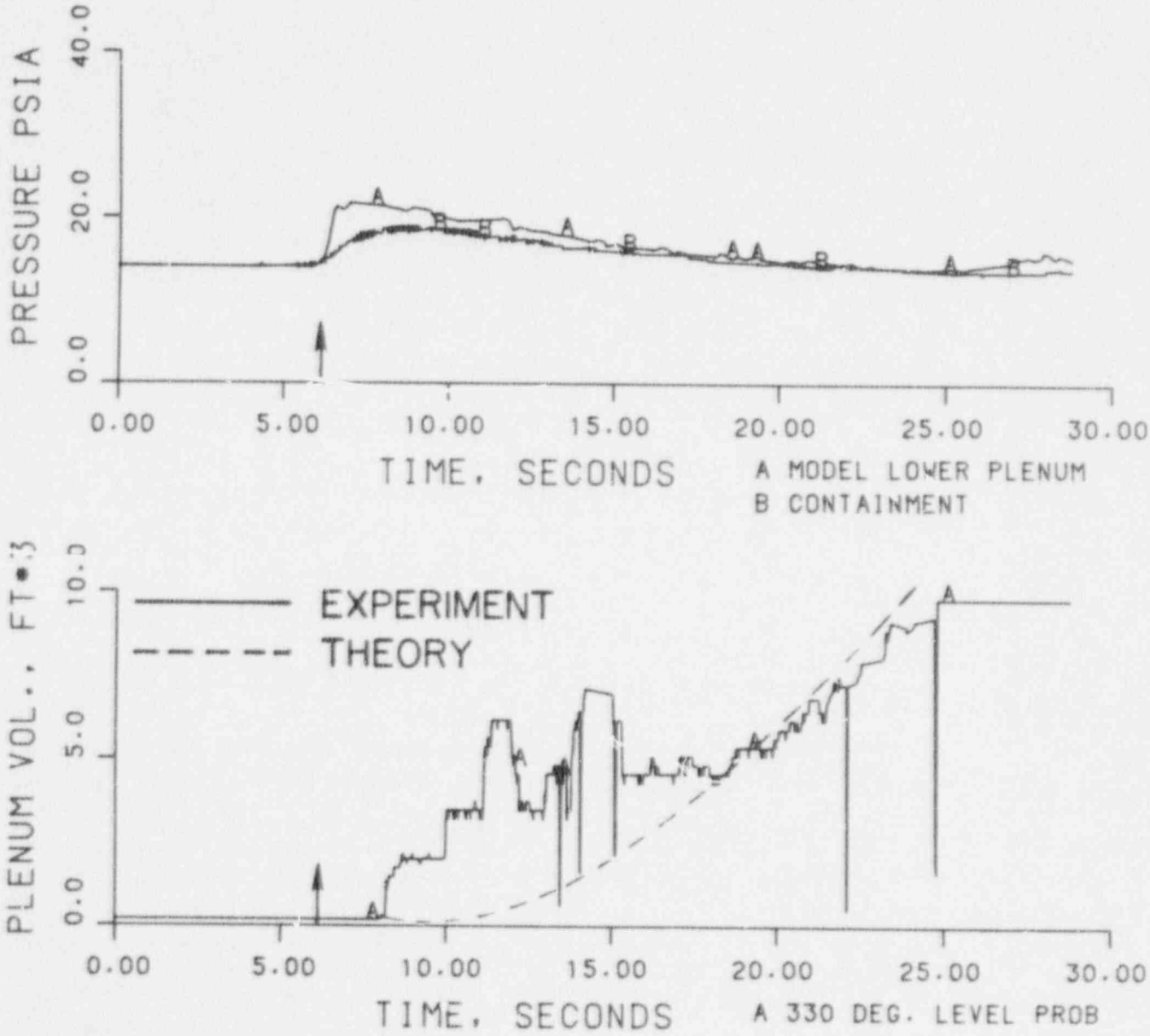

Figure 14. Theoretical and Experimental Results of Test 30202

RUN 30303
T_w = 199 °C
T_{ECC} = 78.3 °C
P_v = 0.11 MPa
K^*_{gc} = 0.0
$K^*_{\ell in}$ = 2.57

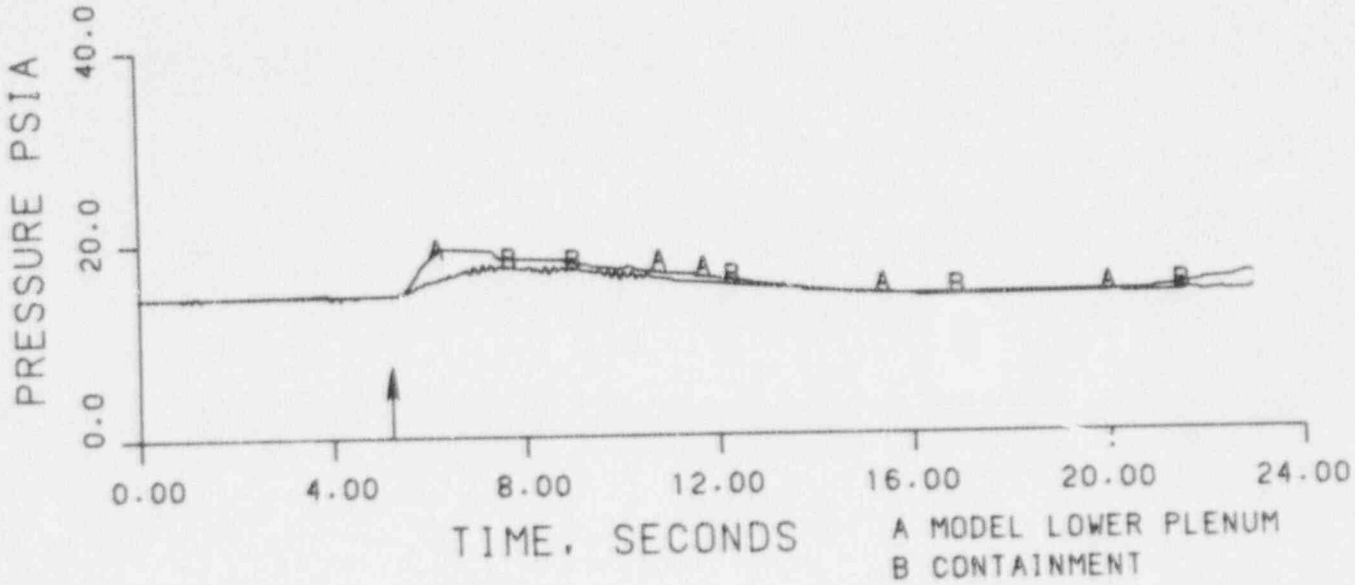

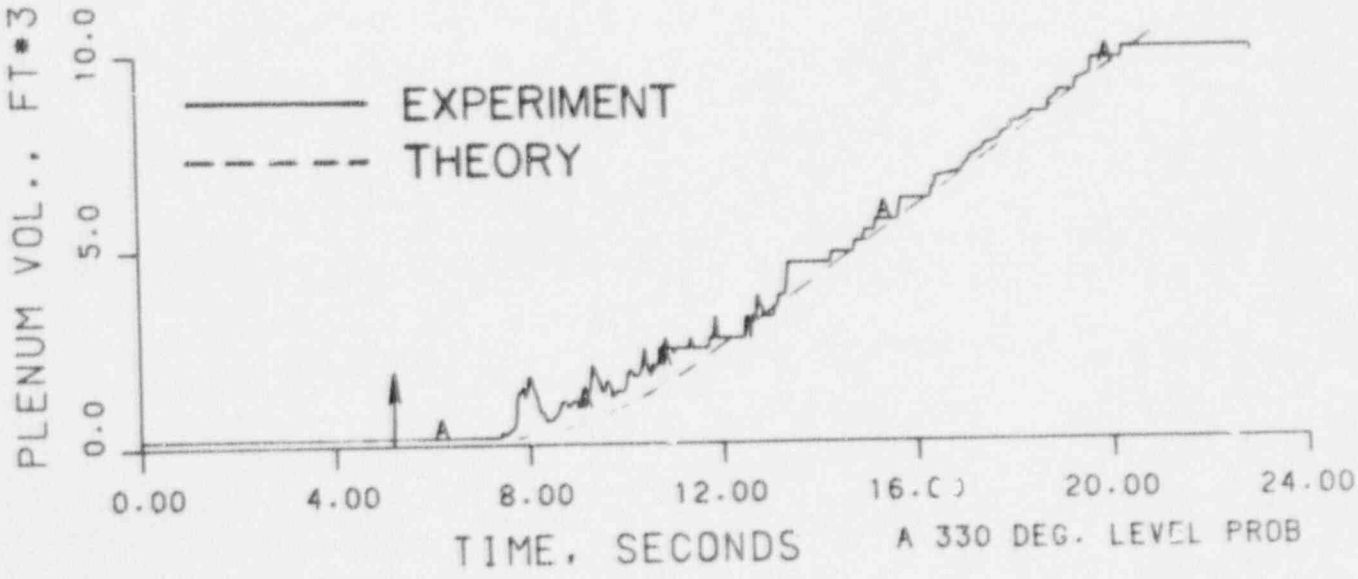

Figure 15. Theoretical and Experimental Results of Test 30303

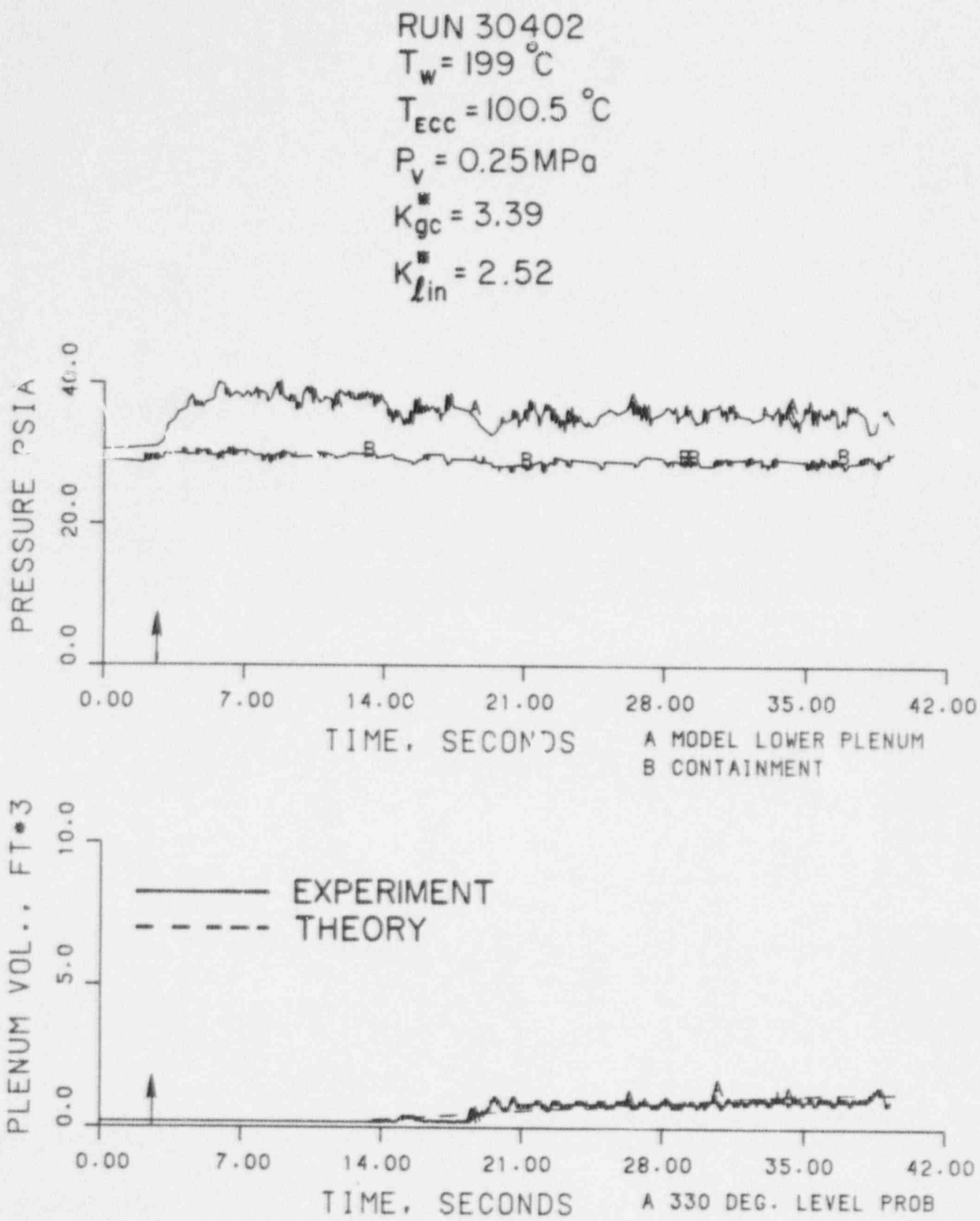

Figure 16. Theoretical and Experimental Results of Test 30402

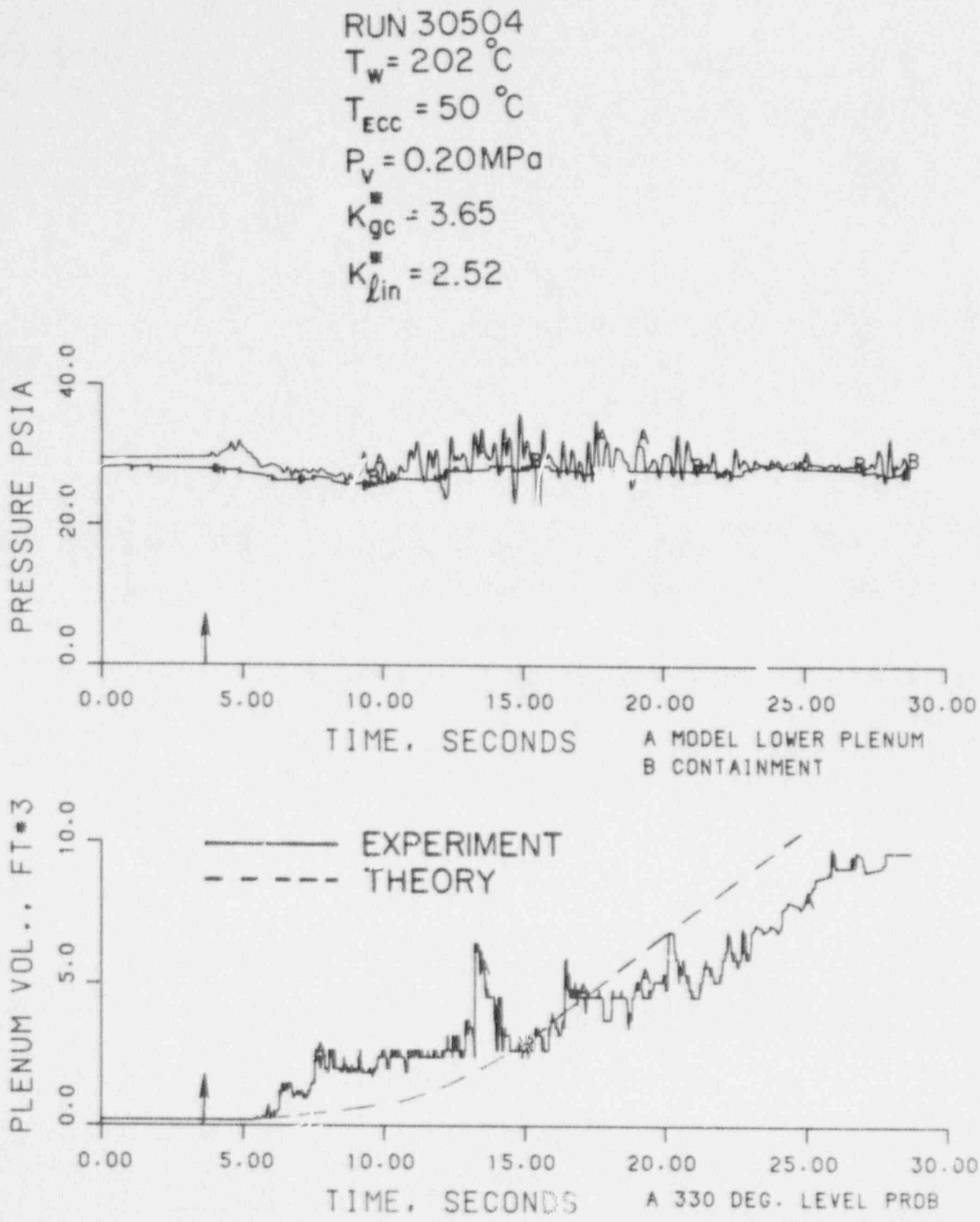

Figure 17. Theoretical and Experimental Results of Test 30504

RUN 30802
T_w = 221 °C
T_{ECC} = 51.1 °C
P_v = 0.20 MPa
K^*_{ℓ} = 3.06
$K^*_{\ell in}$ = 2.52

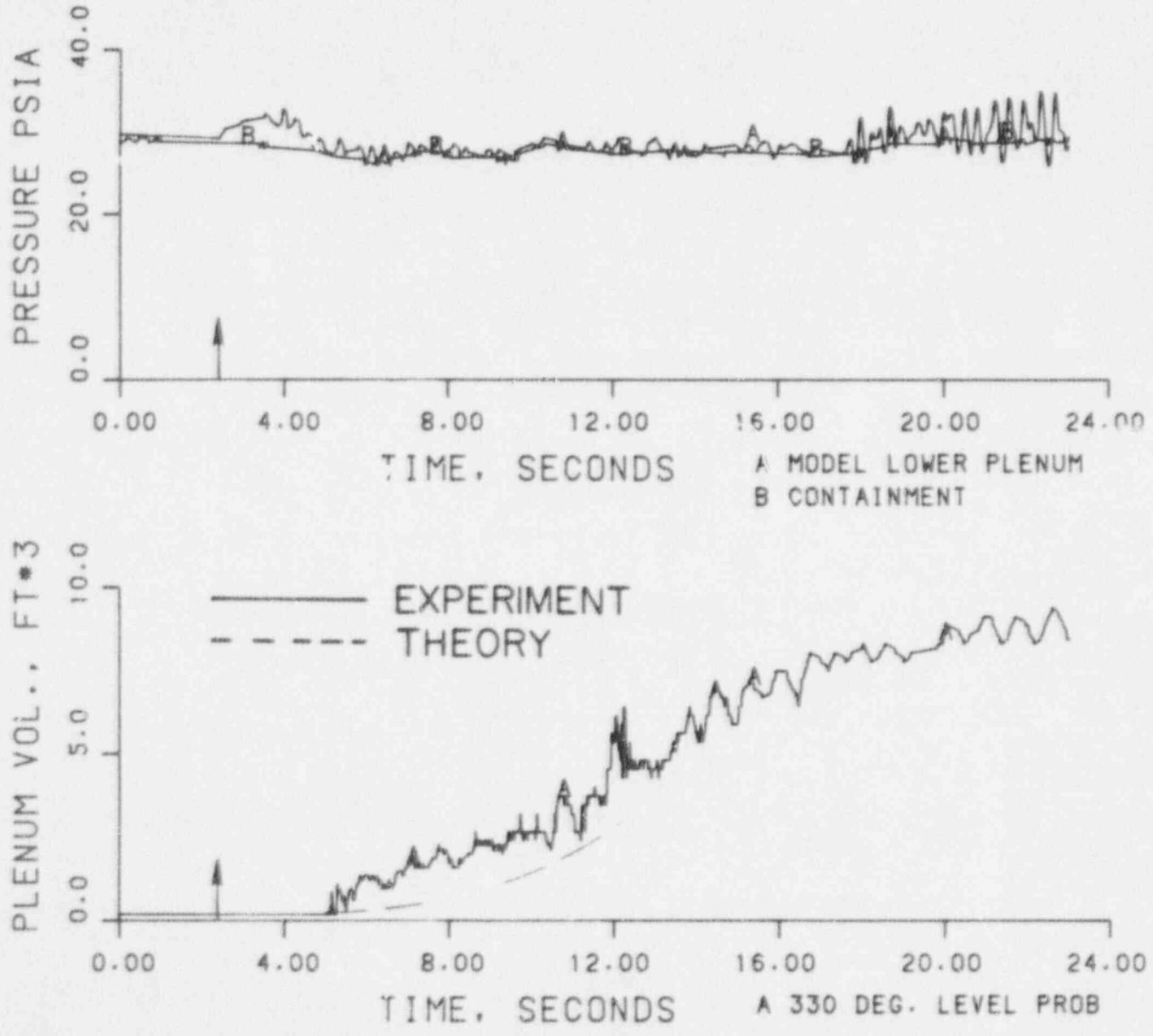

Figure 18. Theoretical and Experimental Results of Test 30802

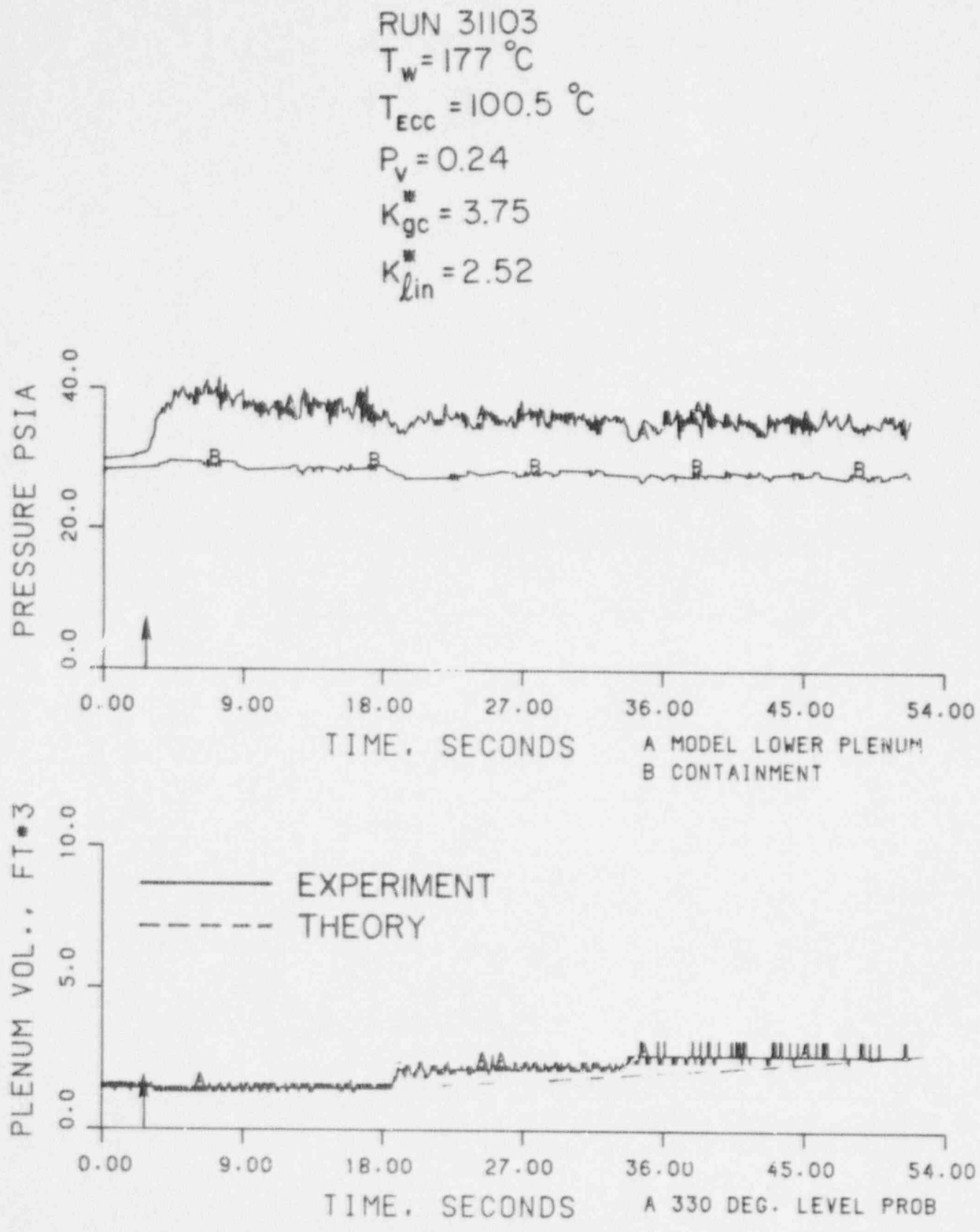

Figure 19. Theoretical and Experimental Results of Test 31103

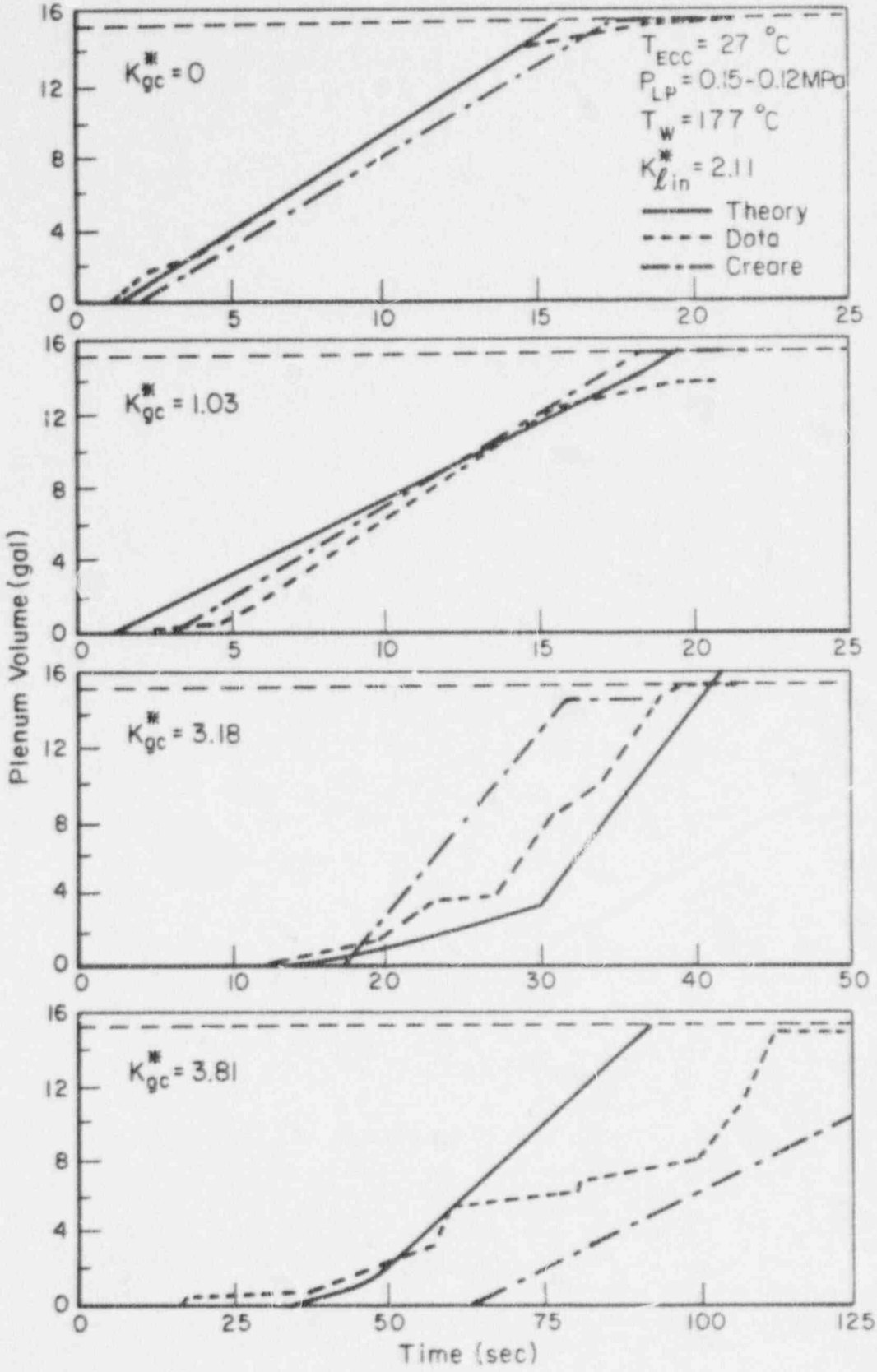

Figure 20. Predicted Filling Trace in Creare's 1/15-Scale Model With a Cold Plenum at TECC = 27 C

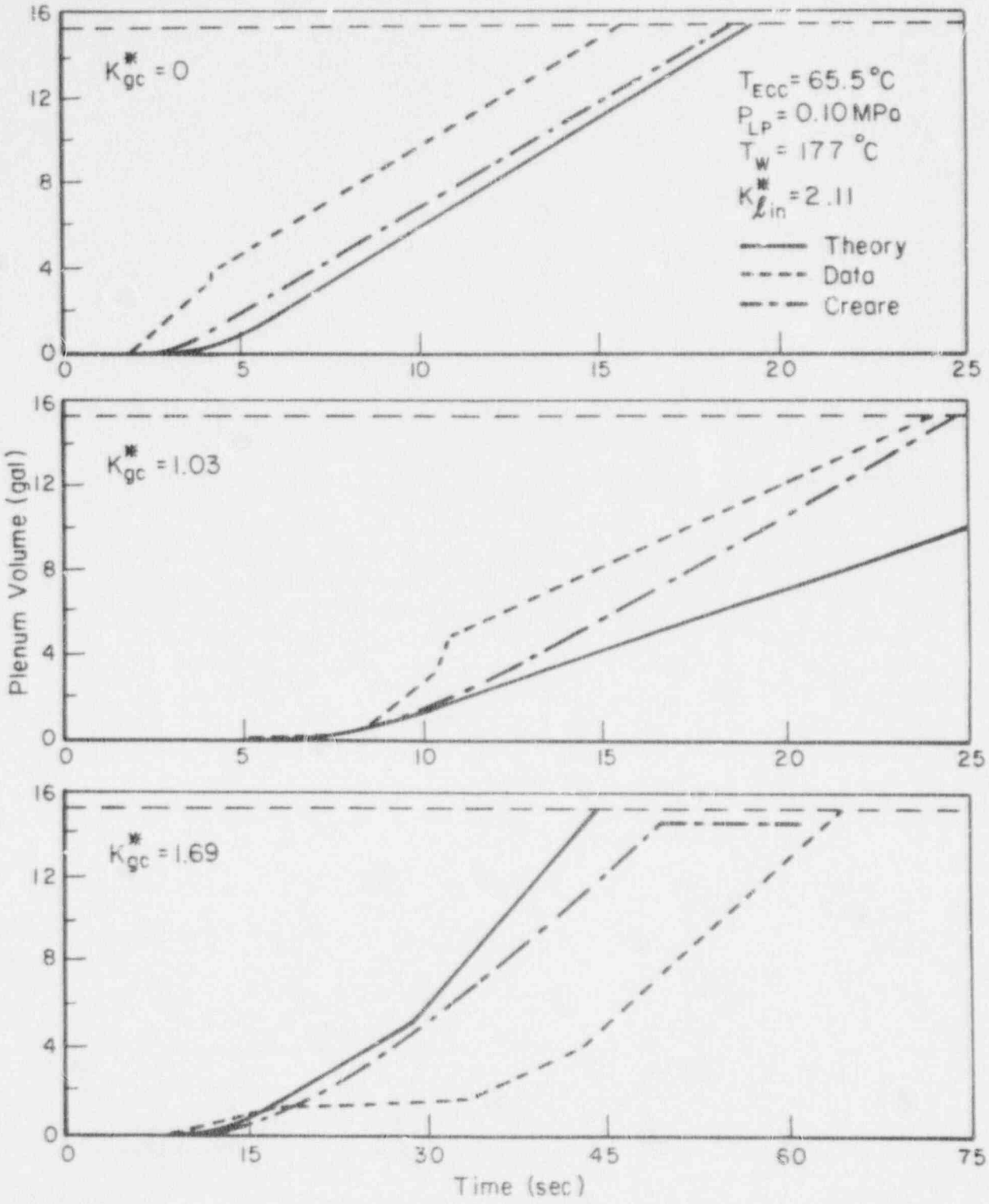

Figure 21. Predicted Filling Trace in Creare's 1/15-Scale Model With a Cold Plenum at TECC = 65.5 C

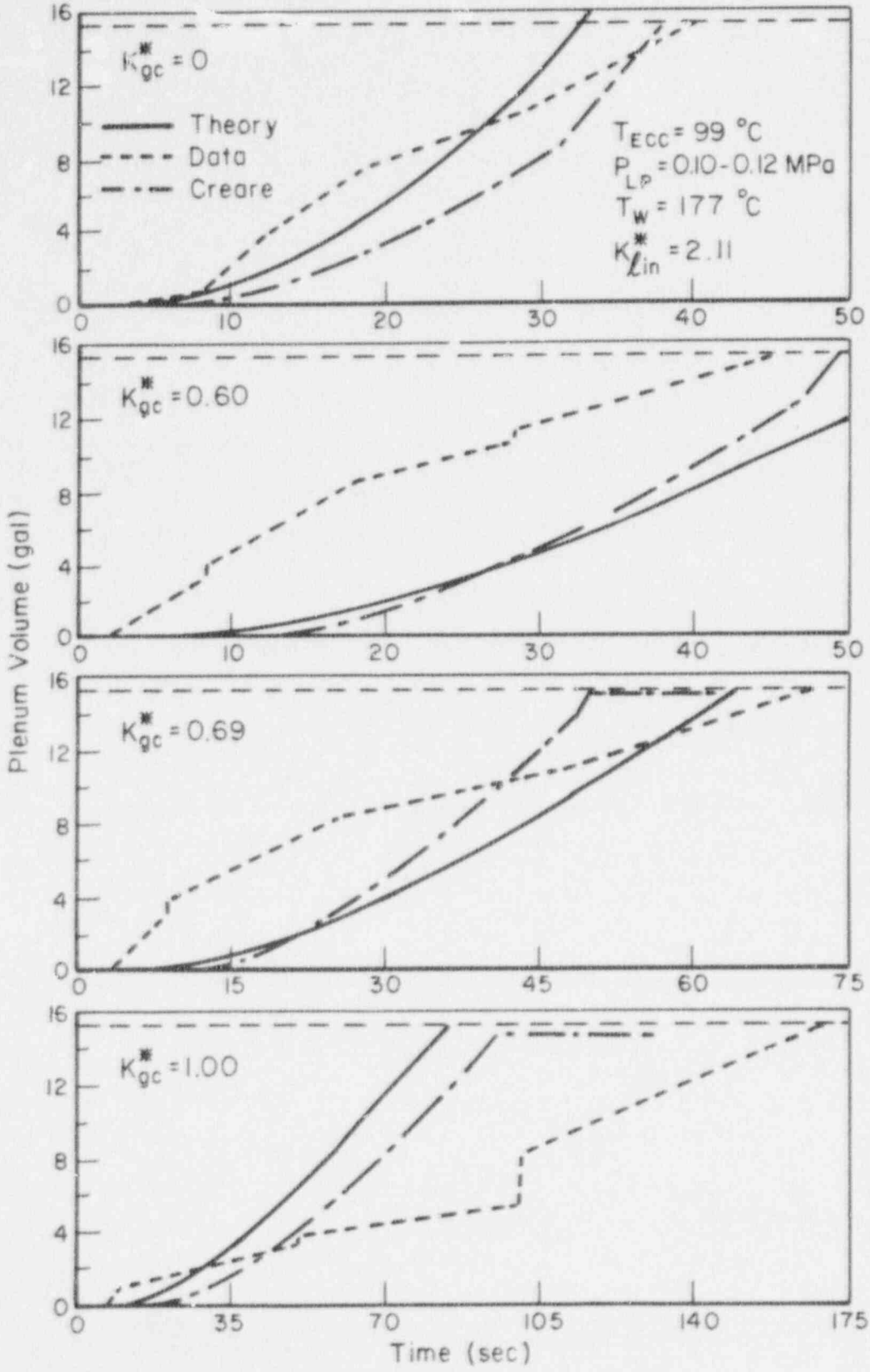

Figure 22. Predicted Filling Trace in Creare's 1/15-Scale Model With a Cold Plenum at TECC = 99 C

the inlet liquid flux is $K^*_{\ell in} = 2.11$. For each ECC temperature, results with several values of constant steam flux are shown. In general, both theoretical models are in reasonably good agreement with the cold lower plenum data.

The next series of tests were conducted with a hot lower plenum. In these tests, the lower plenum and the downcomer walls were heated up to a predetermined temperature and no effort was made to cool down the lower plenum before a test. The hot plenum may result in additional steam generation in the system. It may cause longer delay times and lower penetration rates in comparison to tests conducted with cold lower plenum. To predict the available data with the mechanistic model, a lower plenum heat transfer subroutine was developed. In this subroutine, the heat transfer from the walls is assumed to be conduction limited and the total lower plenum area is considered as the heat transfer area. Also, the boiling in the lower plenum is assumed to be in equilibrium.

Predictions of several filling curves are shown in Figures 23 - 25 for liquid temperatures of 27, 65.5 and 99 C. As shown, the lower plenum heat transfer effect on time delay is well modeled by the mechanistic model. Even for the low liquid subcooling tests, which frequently present a special problem, the time delay predictions are reasonably good. Penetration rates are also well predicted by the theoretical model. The only disagreement between the experiments and the theory is the shift from the transient to the steady-state penetration, predicted to occur sooner than the experimental one.

When the same data are compared with Creare's best estimate model, we note that the delay times predicted are relatively longer than the experimental one and therefore, do not match the early filling. However, the overall time to fill the plenum as well as the steady penetration rates are predicted reasonably well.

Experiments with elevated pressures shown in Figures 26 and 27 with liquid temperatures of 100 C and 146 C (subcooling of about 50 C and nearly saturated, respectively). The comparison with the mechanistic model shows the same trends as observed before. The predicted delay times are in

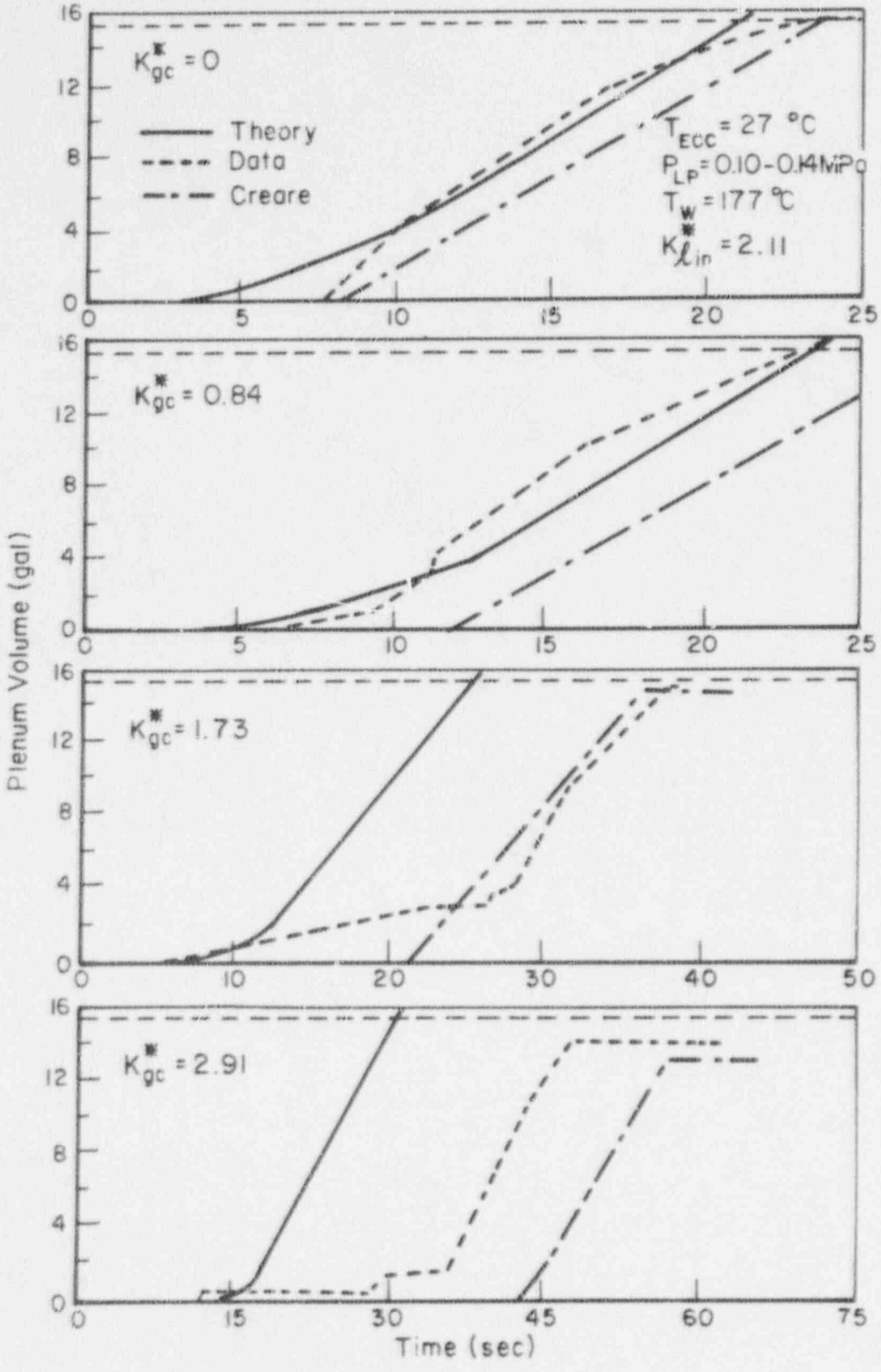

Figure 23. Predicted Filling Trace in Creare's 1/15-Scale Model With a Deep Plenum at T_{ECC} = 27 C

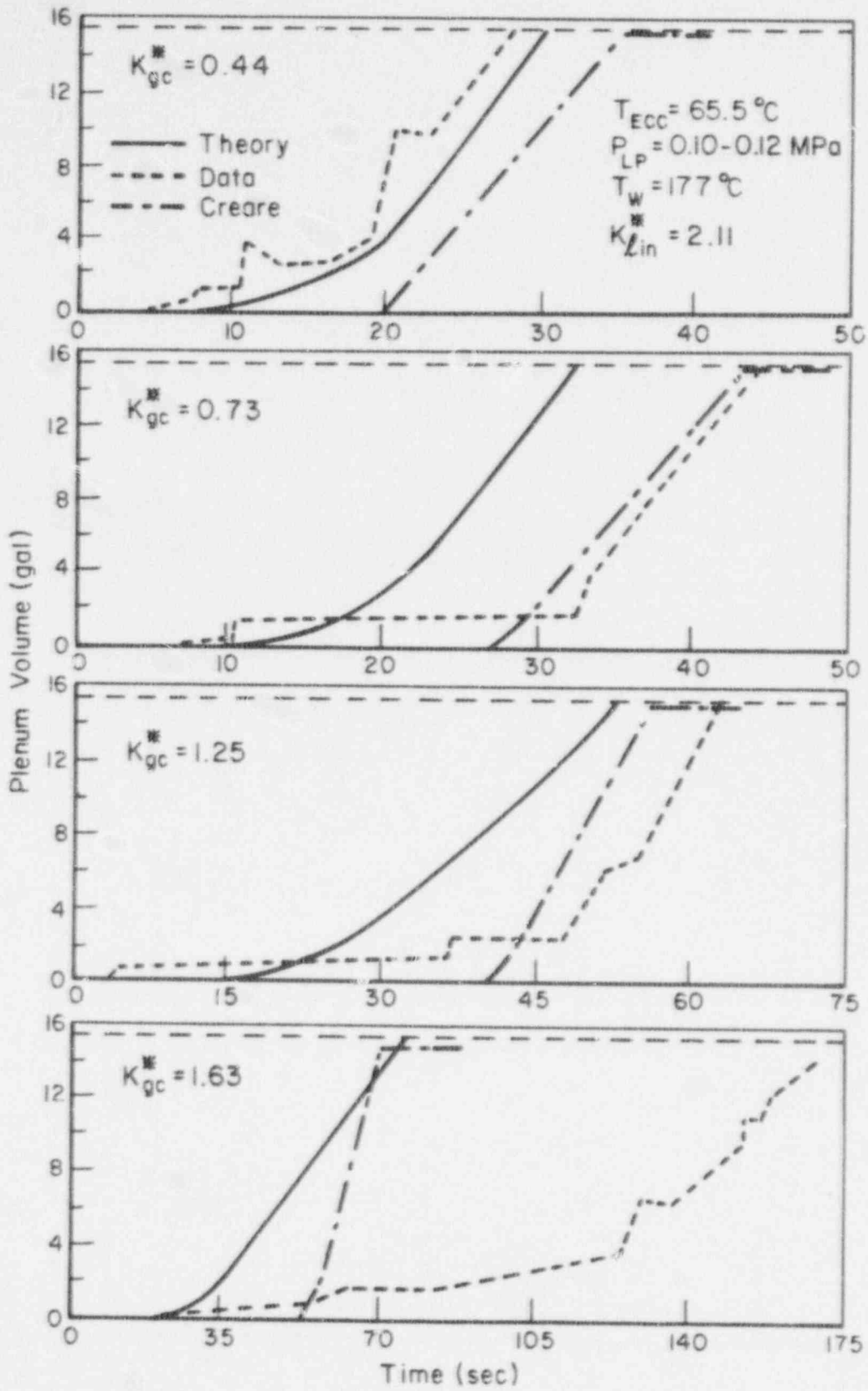

Figure 24. Predicted Filling Trace in Creare's 1/15-Scale Model With a Deep Plenum at TECC = 65.5 C

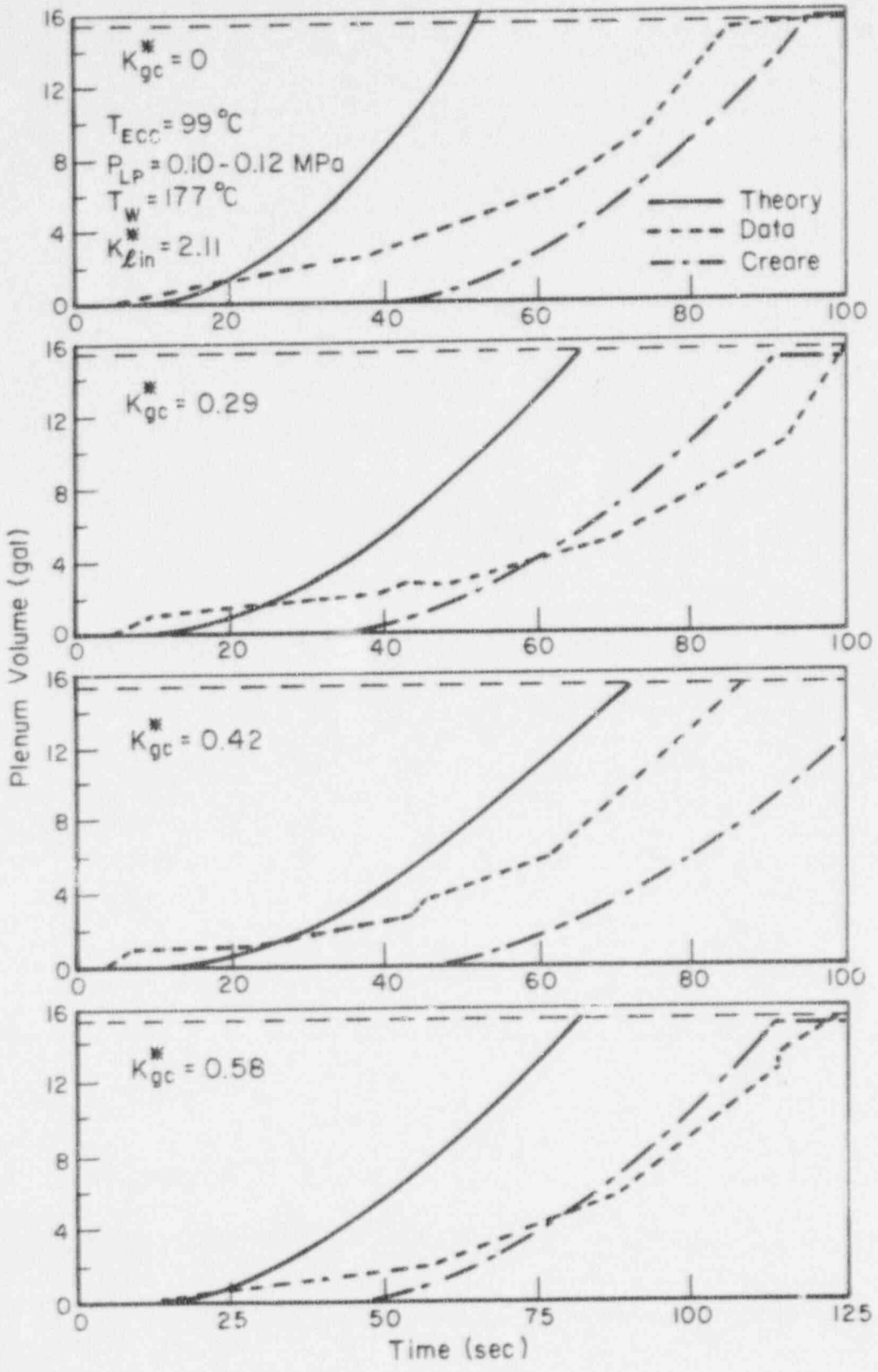

Figure 25. Predicted Filling Trace in Creare's 1/15-Scale Model With a Deep Plenum at TECC = 99 C

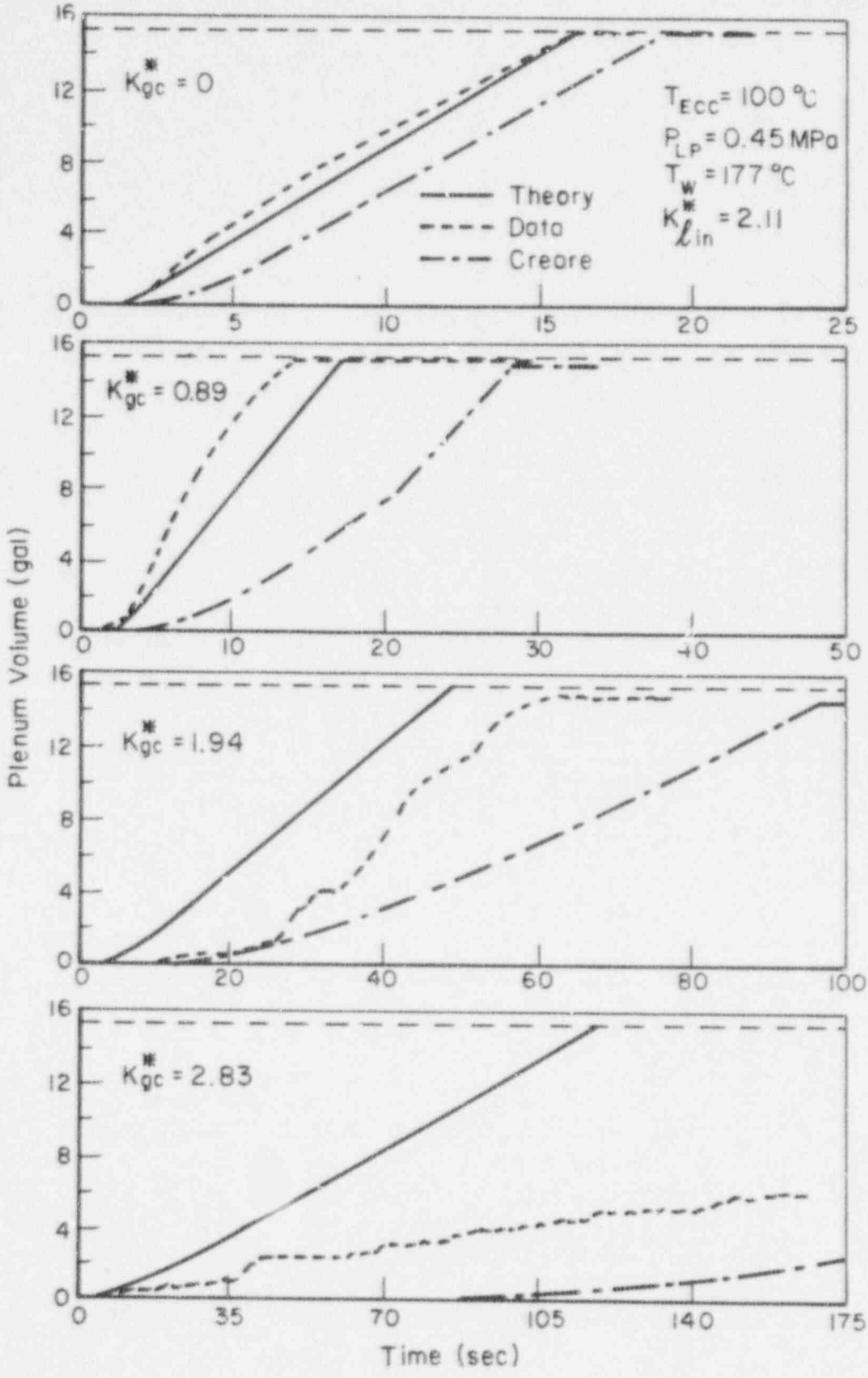

Figure 26. Predicted Filling Trace in Creare's 1/15-Scale Model With a Deep Plenum at 0.45 MPa and TECC = 100 C

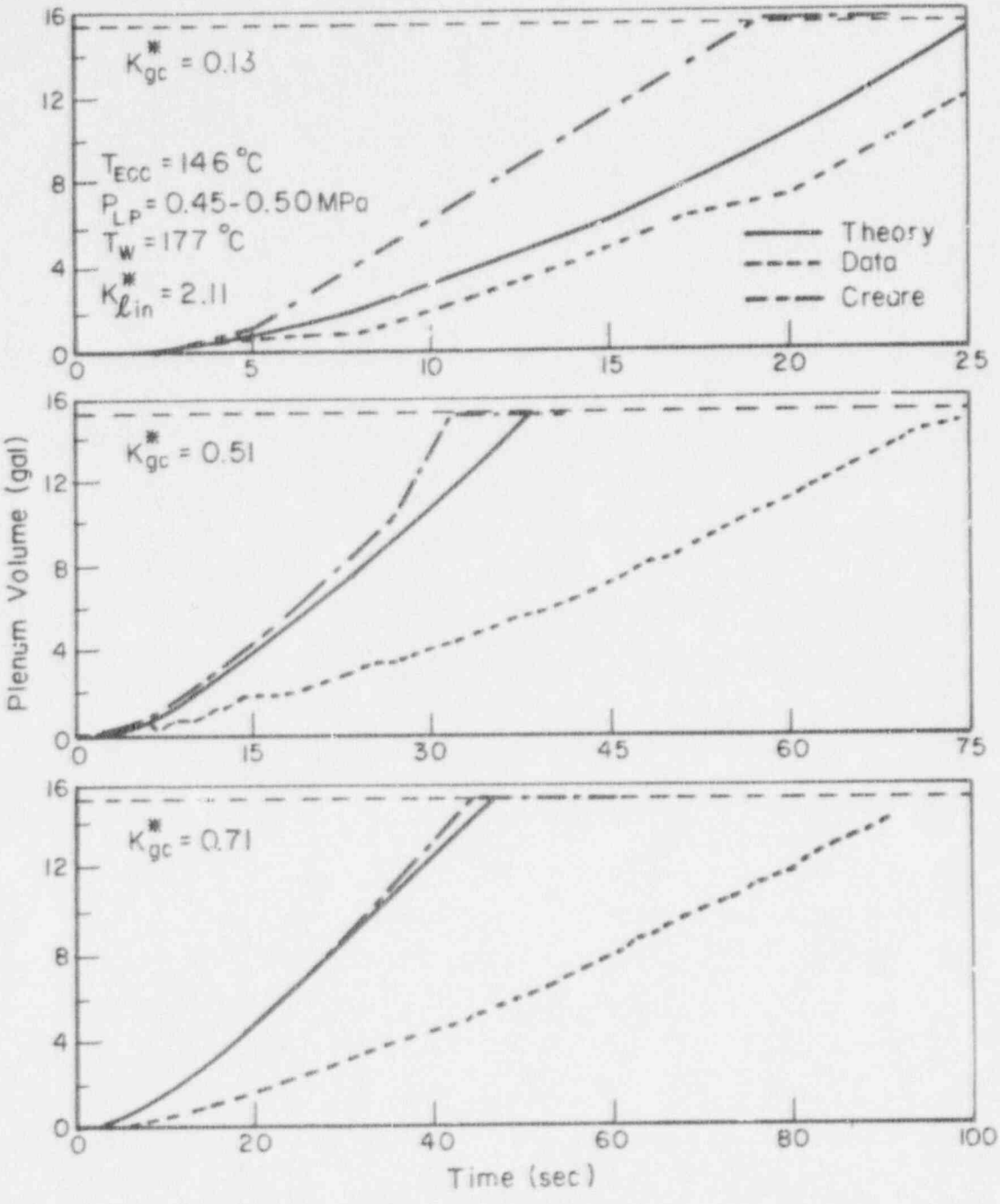

Figure 27. Predicted Filling Trace in Creare's 1/15-Scale Model With a Deep Plenum at 0.45 MPa and TECC = 146 C

reasonably good agreement with the data, but the plenum filling rates are overpredicted for high steam flows, especially in the saturated liquid case. Creare's best estimate model underpredicts the penetration rates for the subcooled case and overpredicts them for the saturated case.

Figure 28 illustrates the effect of initial wall superheat on plenum filling behavior. Theoretical predictions with two different assumptions are described. One assumes that the lower plenum is hot and contributes to the vapor generation only in the downcomer. For the lower wall temperature (121 C) no difference between the two is observed and the prediction agrees well with the experiment. For wall temperatures of 177 C and higher, the hot lower plenum assumption results in underprediction of the penetration rates and overprediction of the time delays. This becomes more pronounced as the wall superheat increases. The same trends are also evident in Creare's predictions. A better agreement is observed when the penetration is predicted by the mechanistic model with the colder lower plenum assumption. This is similar to the results obtained for the 2/15-scale model[21] where the predicted penetration curves were in better agreement with data when a cold lower plenum was assumed.

From the experimental data and from the theoretical model we can evaluate the effects of the major variables on the plenum filling behavior.

Core Steam Flow - As core steam flow rate increases more liquid is bypassed, resulting in a longer delay time, a longer period of steam generation, and lower rate of steady penetration.

ECC Water Flow - The major effect of inlet liquid flow rate is on the condensation on the bypassed liquid (K^*_{cbp}). As $K^*_{\ell in}$ increases, K^*_{cbp} increases and consequently $K^*_{\ell i}$ increases, resulting in shorter time delays, a shorter transient period, and a larger steady penetration rate.

ECC Subcooling - Subcooling ($\Delta T_s = T_s - T_{\ell i}$) affects the condensation potential and net vaporization point z_o. An increase in ΔT_s results in an increase in condensation and z_o. The latter indicates that the boiling component of the wall heat flux decreases as liquid subcooling increases. This also can be shown from the expression f, Equation (26). All of these processes cause enhancement of liquid penetration.

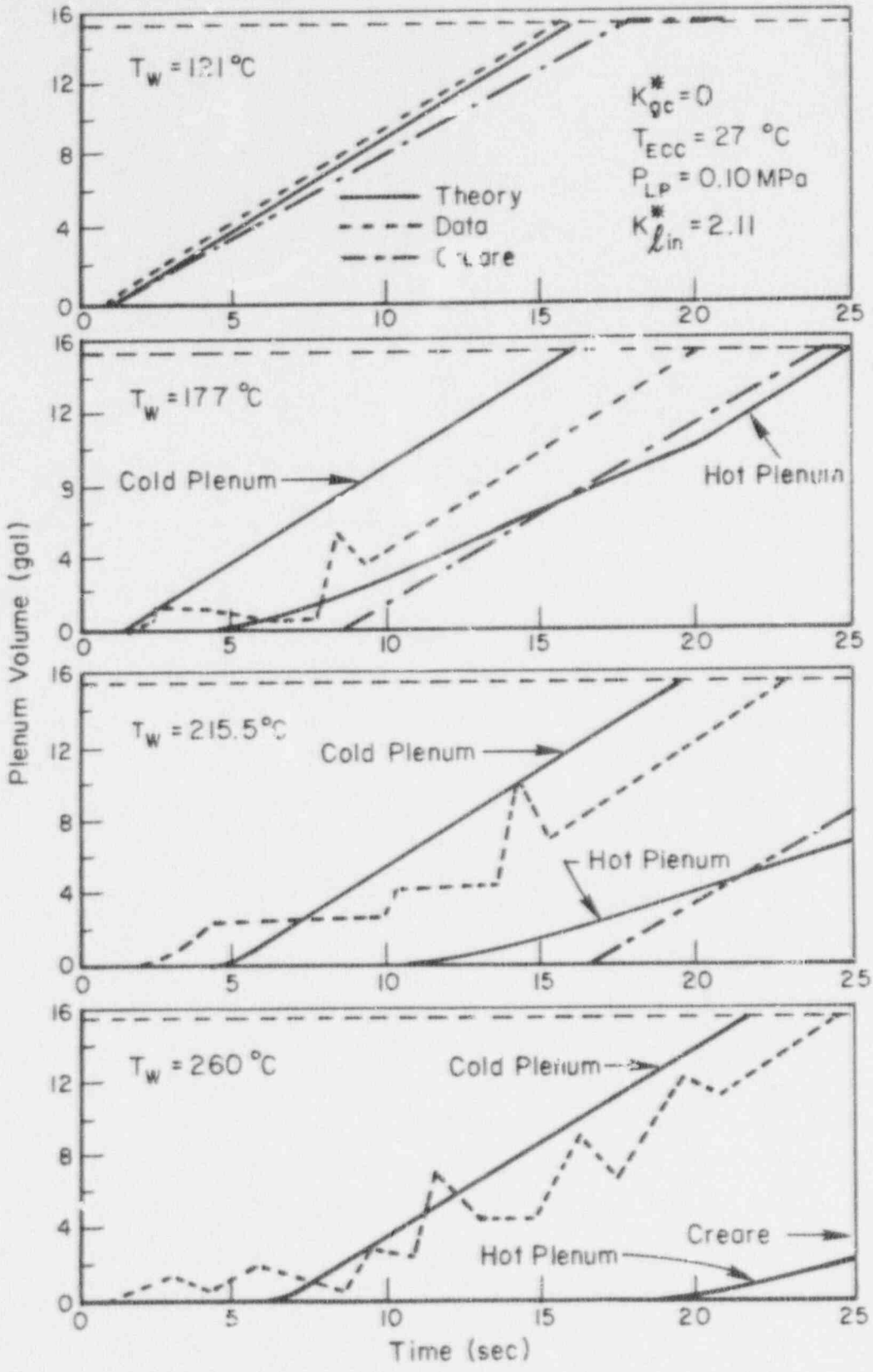

Figure 28. Predicted Filling Trace in Creare's 1/15-Scale Model With a Deep Plenum at Various Wall Temperatures

Pressure - As the pressure in the vessel increases, liquid subcooling increases, wall superheat decreases, and the effective dimensionless steam flux decreases, all resulting in faster filling of the lower plenum.

Wall Superheat - ($\Delta T_w = T_w - T_s$) When the wall superheat increases, more vapor is generated. If the pressure remains unchanged, the vapor generated increases the effective steam flow and the filling of the lower plenum is delayed. However, if the pressure in the lower plenum increases due to the enhanced vapor generation, the filling rate may increase and the time delay may decrease according to the pressure effects discussed above.

Predictions of thermal-hydraulic behavior in PWR's during a LOCA show that reverse core steam flow and pressure will vary with time before and during ECC injection. Typical examples of such calculated transients are presented in Section V where the present analysis is applied to a full scale PWR.

Transient experiments have been conducted in 1/15-[2] and 2/15-[1] scale models in which various transients in the core steam flow and the vessel pressure were produced with different initial conditions. Usually in these experiments the reverse core steam flow is held initially at some high value and then it is ramped to zero at a controlled rate, by closing a control valve. A detailed discussion of the experimental results, data trends, and the effects of various parameters on the filling rate can be found in References 2 and 3.

We have shown that the mechanistic model may be applied to ramped steam flow experiments [8] by assuming that the penetration process is in a pseudo-steady state. Comparison with experiments in the 1/15-scale model of Creare resulted in very good agreement [8] but the comparison with the 2/15-scale model experiments was not as good. It was hypothesized that the disagreement was probably because the liquid film does not fill the annulus, as was assumed. In the present modified mechanistic model, the film thickness is obtained from the Nusselt equation. As a result, the modified model predicts the filling curves better, as shown in Figures 29 and 30.

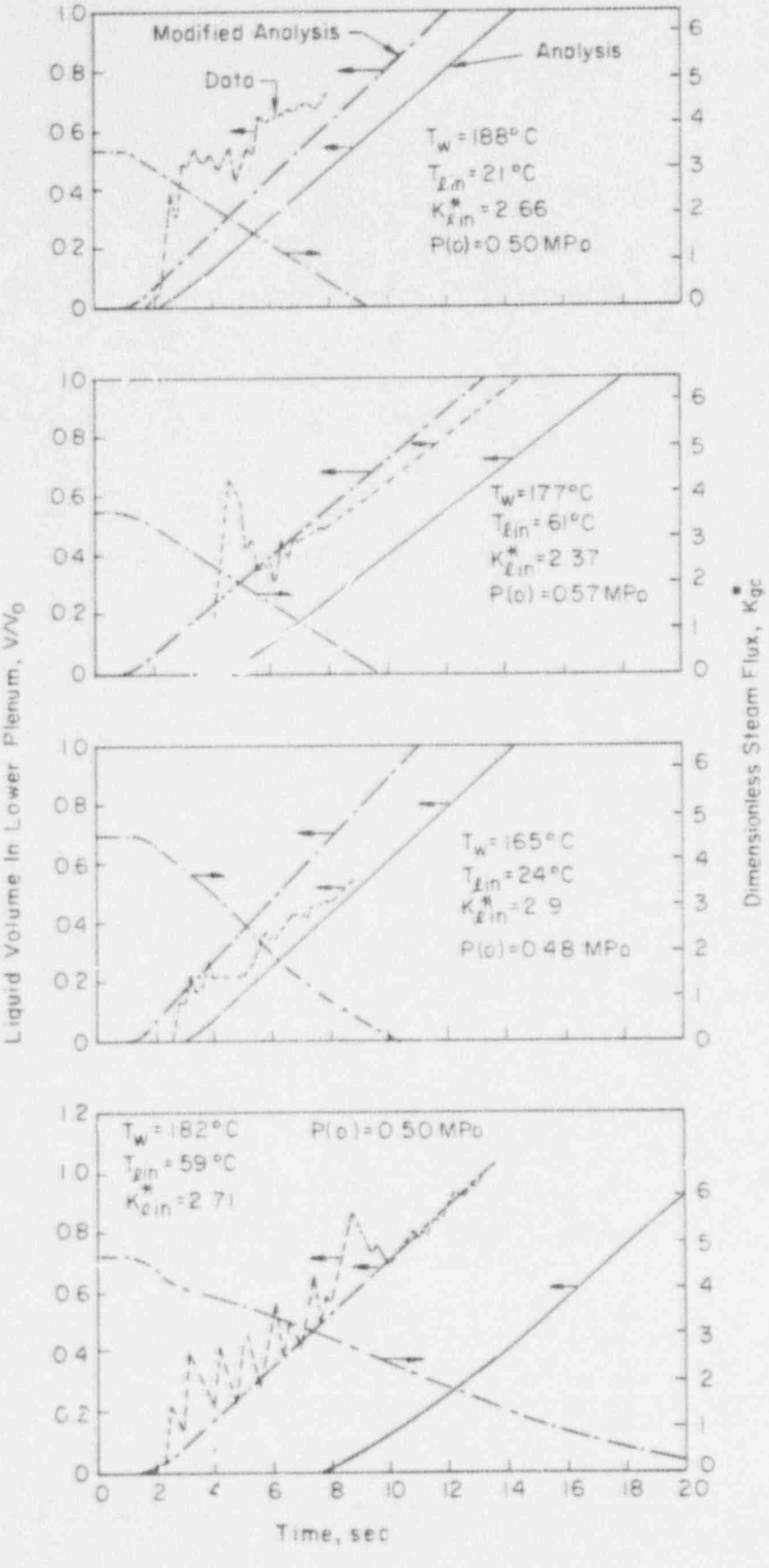

Figure 29. Comparison Between Experimental and Theoretical Plenum Filling in Battelle's 2/15 Scale Model With Ramped Steam Flow

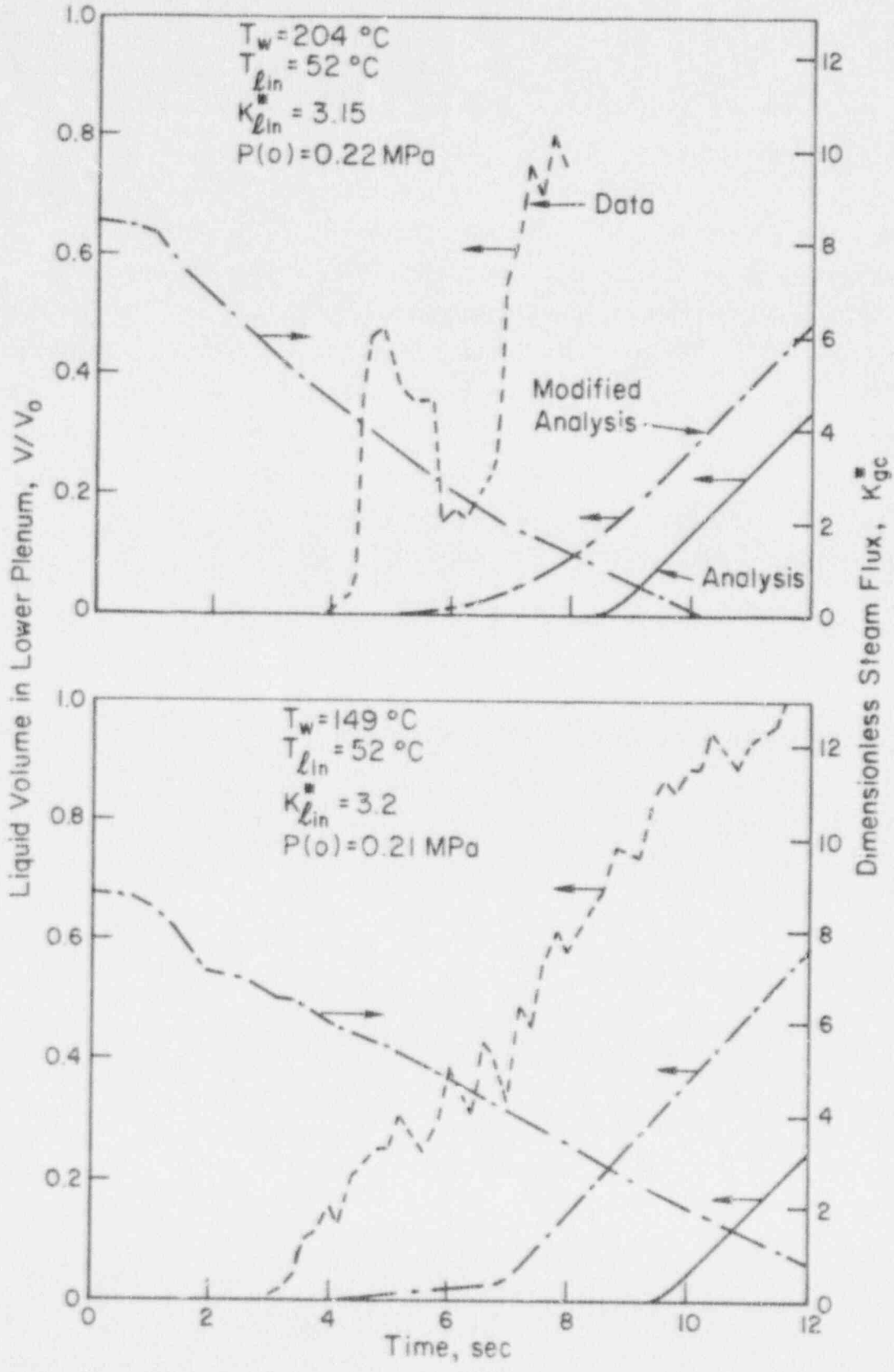

Figure 30. Comparison Between Experimental and Theoretical Plenum Filling in Battelle's 2/15-Scale Model With Ramped Steam Flow

The mechanistic model was also applied to some recent experiments conducted in the 2/15-scale model. These ramped steam flow tests were performed with and without superheated walls. Figures 31 - 34 show some comparisons between the calculated and experimental filling traces of these tests. As shown, the delay times and penetration rates are predicted reasonably well by the modified mechanistic model. It should be noted that the lower plenum is assumed to be "cold", as was done when steady-state hot wall experiments were considered. Also, in the case of short transients, a situation may occur in which the transient in steam flow rate is over (i.e., $K^*_{gc} = 0$) while the liquid is still in the annulus. In this case we assume that the liquid falls freely to the lower plenum. This assumption is supported by the experiments conducted in the 2/15-scale model with superheated walls and no core steam flow ($K^*_{f,c} = 0$) in which the measured time delays were near the free fall time.

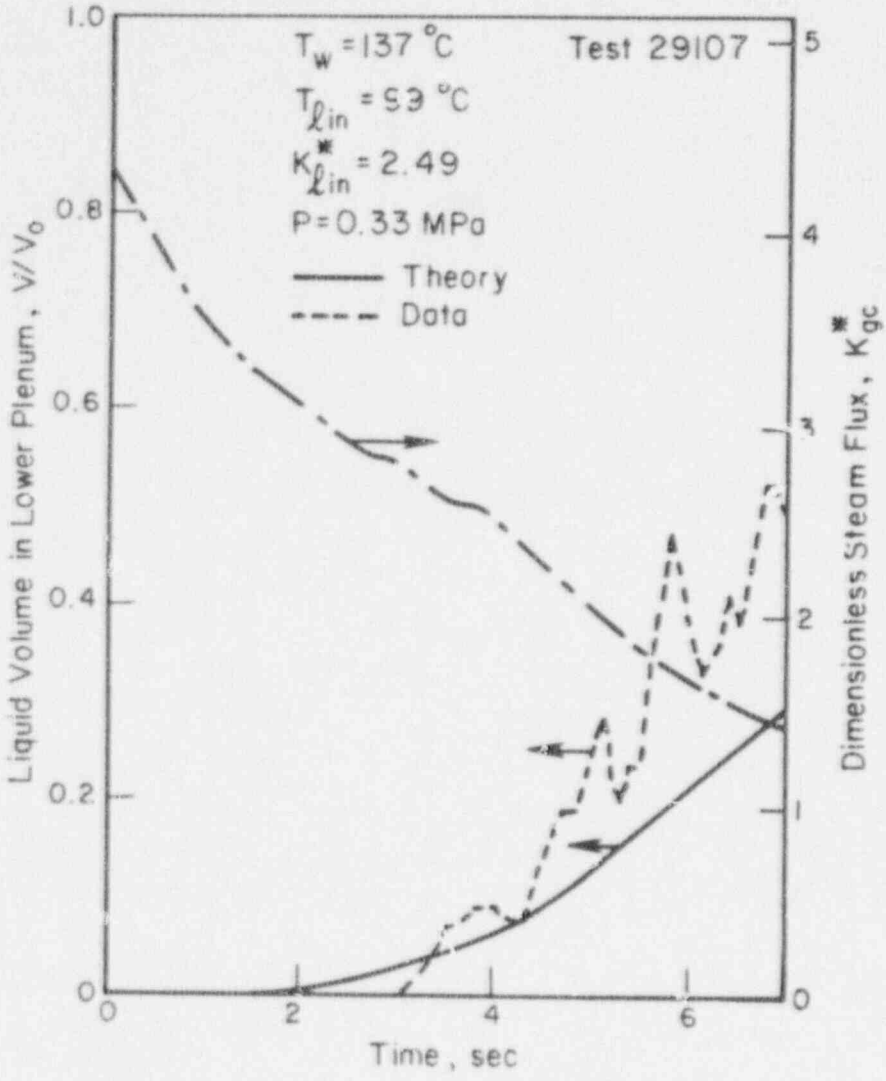

Figure 31. Predicted Filling Trace of Test 29107

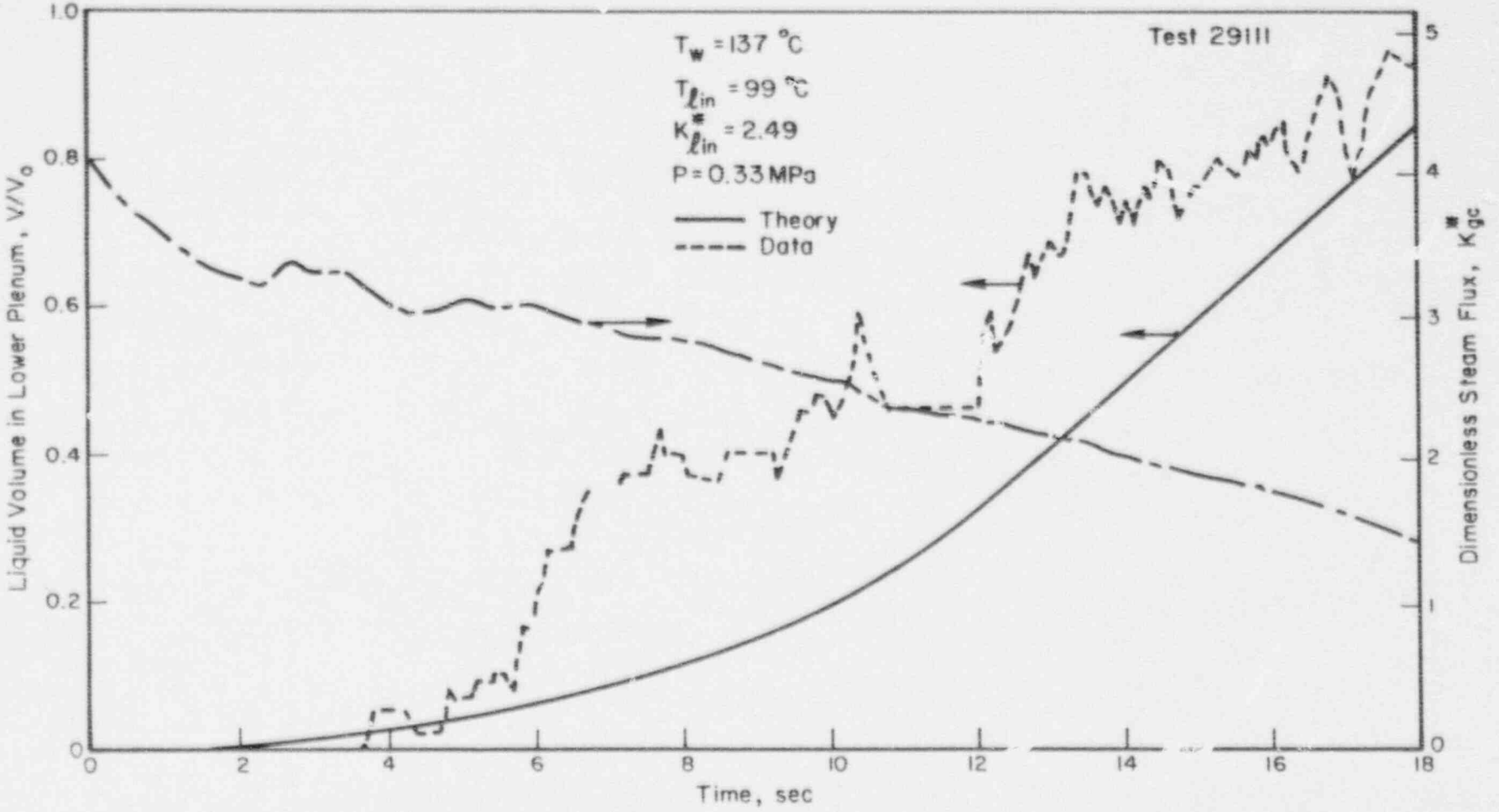

Figure 32. Predicting Filling Trace of Test 29111

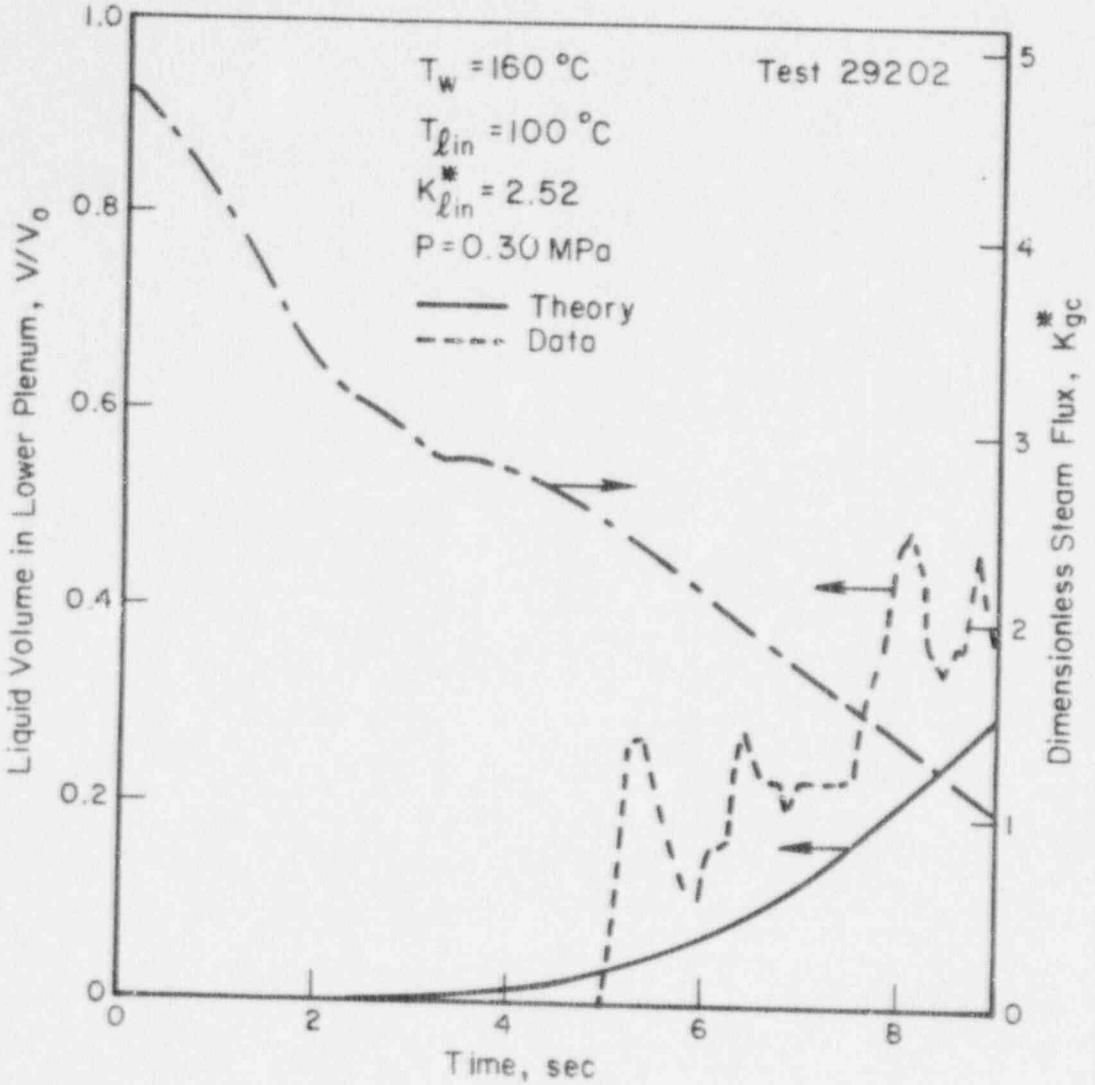

Figure 33. Predicted Filling Trace of Test 29202

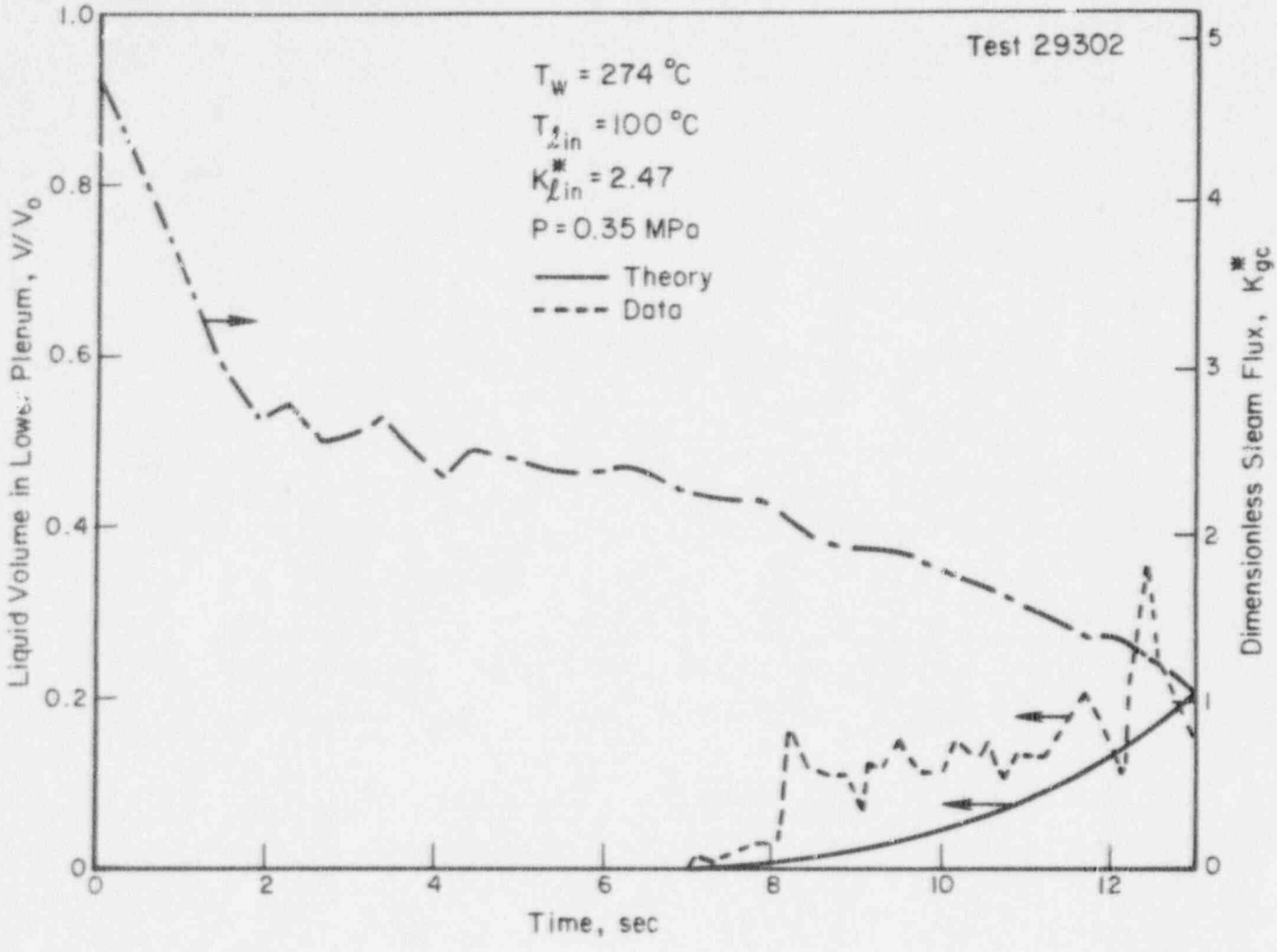

Figure 34. Predicted Filling Trace of Test 29302

IV. ECC PENETRATION IN LOFT TEST L1-4

This section compares analysis and experimental measurement of lower plenum filling for Test L1-4[22] of the Loss-of-Fluid Test (LOFT) Program[23]. The LOFT facility is a scale model of a PWR with a volume scaling ratio of approximately 1 to 60. Its downcomer is approximately full scale in the axial direction and approximately 1/5 linearly scaled in the radial direction. The pertinent dimensions of the LOFT vessel are listed in Figure 1.

Test L1-4 was the fourth in a series of five non-nuclear isothermal tests performed as part of the LOFT integral test program. This experiment was chosen for comparison with our analysis because it is a double ended blowdown with ECC injection and because extensive information is available in terms of experimental data[22] and code calculations using RELAP[24,25] and TRAC[26].

Except for the downcomer steam flow rate information, the LOFT data generally meet the input requirements for the transient plenum filling analysis. Figure 35 describes the time dependent values of vessel pressure, temperature of the mixture entering the upper annulus, and the ECC flow rate which were obtained in Test L1-4 and used in our calculations. The transient reverse core steam flow used in the analysis has been calculated in Reference 27 and is given here in a dimensionless form in Figure 36.

The experimental filling behavior in Test L1-4 is shown in Figure 37. We note that at the time of ECC injection, about 22 seconds after rupture, the plenum inventory is decreasing due to blowdown. This decrease is observed to last an additional period of 12 seconds (34 seconds after rupture) when the plenum inventory reaches its minimum of about 65 percent of the plenum volume. At that time, which may be regarded as the experimental delay time, the lower plenum beings to fill. The plenum is full approximately 22 seconds after injection began, or 10 seconds after the plenum started to fill, which implies an average filling rate of 0.025m^3 per second (6.5 gallons/sec).

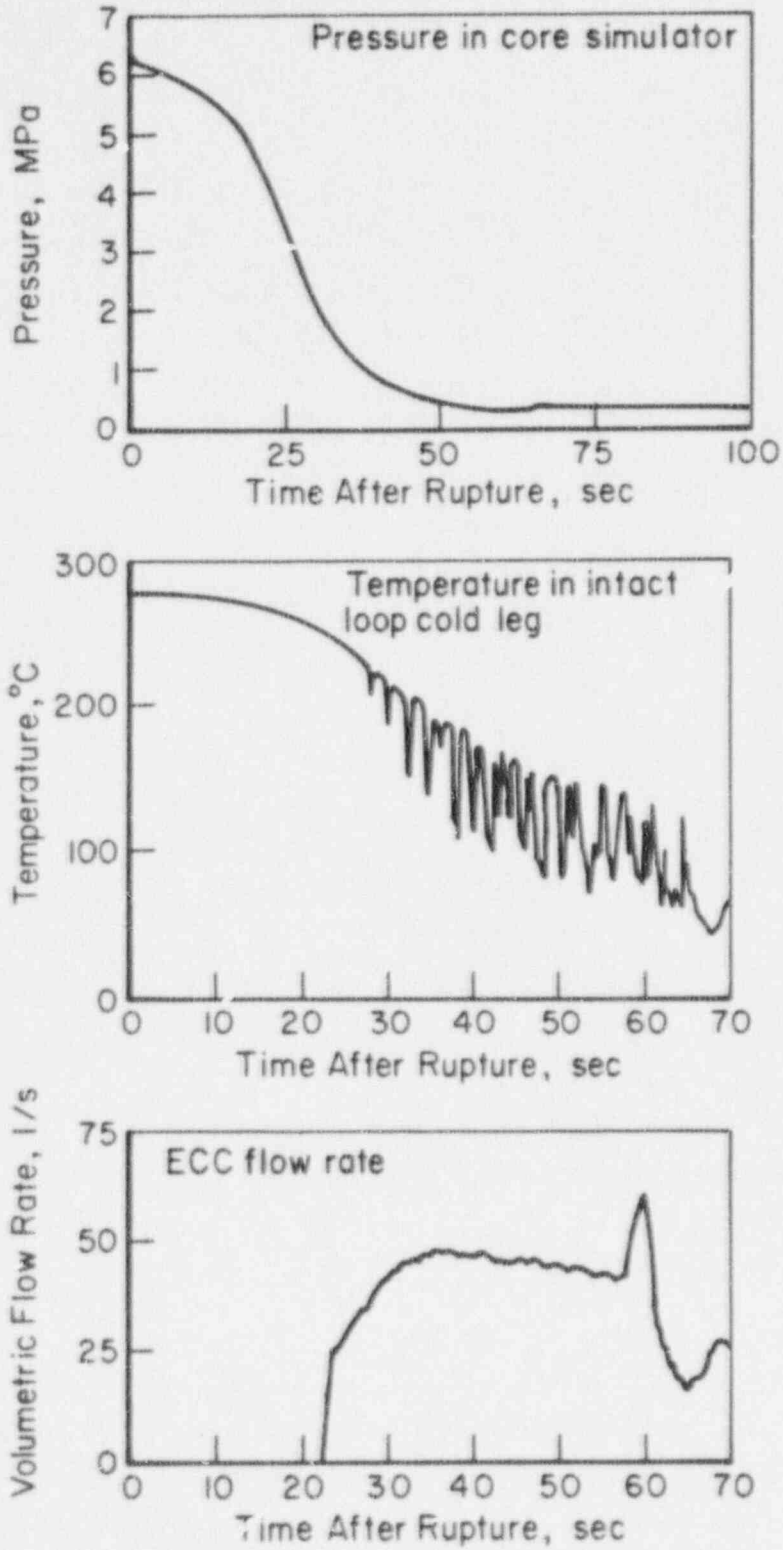

Figure 35. Experimental Conditions in LOFT LOCE L1-4

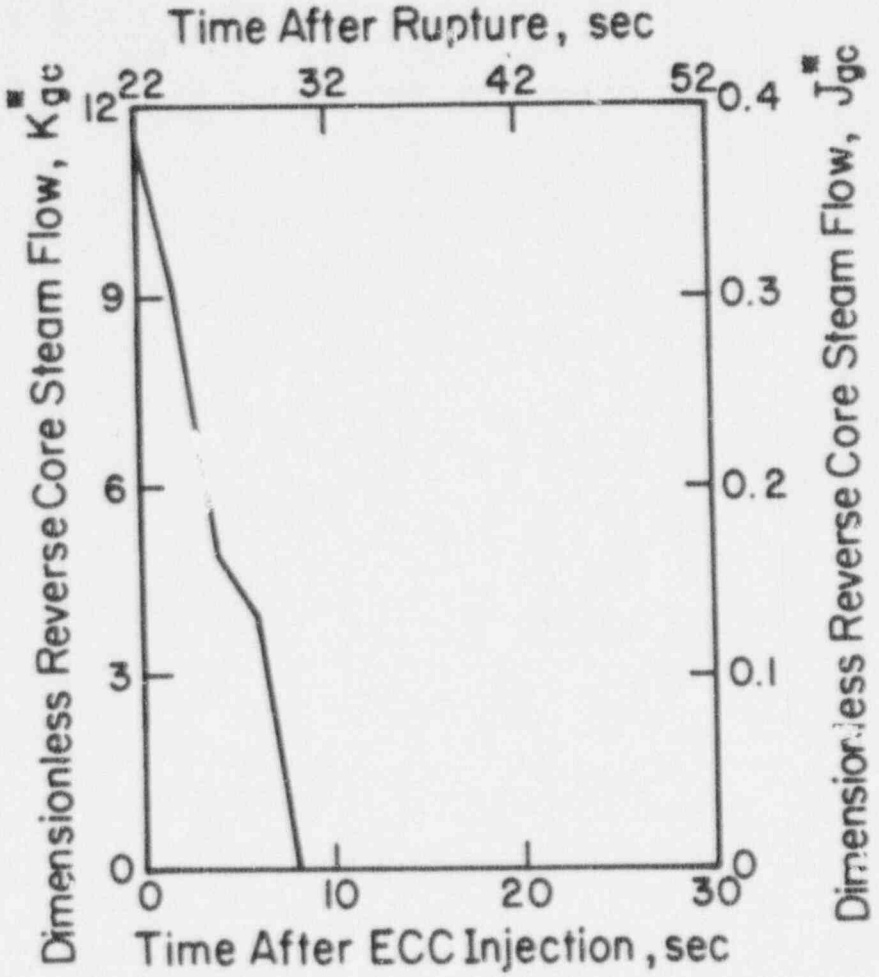

Figure 36. Dimensionless Steam Flow Rate Input (Reference 27)

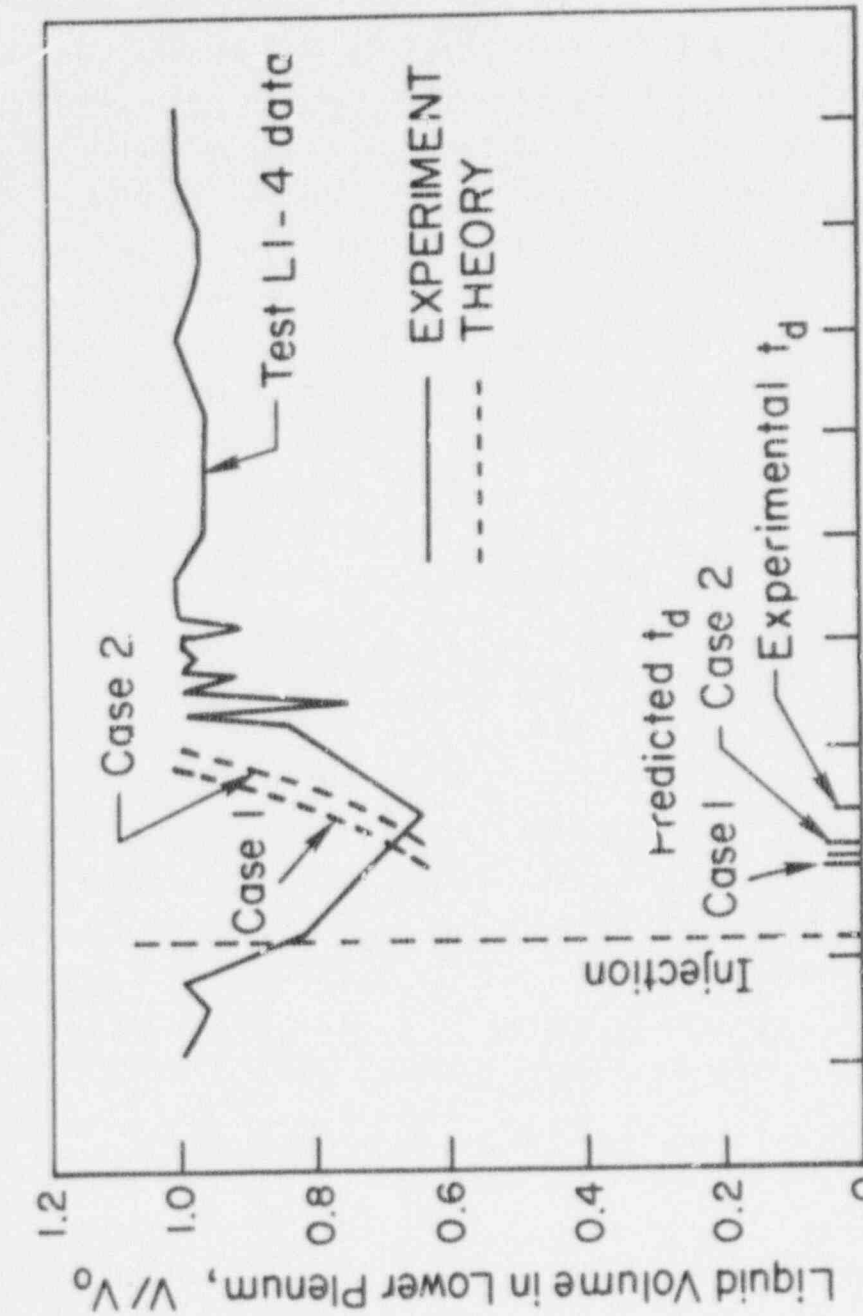

Figure 37. Liquid Volume Fraction in Lower Plenum During LOFT LOCE L1-4

The calculated plenum filling is also shown in Figure 37. Two theoretical cases were evaluated. In Case One, we assume that the film thickness is given by Nusselt equation. In Case Two, we assume that the liquid fills the downcomer as it propagates down. For Case One, the plenum filling is predicted to begin 9.0 seconds after ECC injection, or 3.0 seconds earlier than the experimental value. At 18.0 seconds into the transient, the lower plenum is predicted to be full, implying an average filling rate of $0.026m^3$/sec (6.80 gallons/sec). Thus, excellent agreement is shown between the experimental and the predicted filling rate. For Case Two, the predicted time delay is 1.5 seconds longer than in Case One, i.e., t_d for Case Two is 10.5 seconds. The lower plenum is filled after 19.5 seconds, resulting in the same filling rate as in Case One. It is unclear at present why the predicted time delays in both cases are shorter than the experimental value (it is 25 percent shorter in Case One and 12.5 percent shorter in Case Two). The reason for that may be found in one of the following:

(1) Inaccuracies in the calculated input of the reverse core steam flow to the downcomer may have caused the predicted ramp time to be less than the experimental value.

(2) Significant voiding may have occurred in the lower plenum. This would supply additional steam flow to the downcomer, resulting in longer experimental time delays. This potential voiding was neglected in the present analysis.

(3) Inaccurate measurement of liquid level.

It is interesting to note that the shorter time delay predicted here is consistent with the calculations done with the TRAC computer code, which also underpredicts the time delay by 4 seconds[26].

For the reasons stated above, it is difficult to draw definite conclusions concerning the liquid behavior in the downcomer. However, since the assumption made in Case Two is more conservative and the results obtained are closer to the LOFT experiment, the liquid was assumed to fill the downcomer in the following analysis of a full scale PWR.

V. ECC PENETRATION IN A FULL SCALE PWR

In this section we calculate filling of the lower plenum in a full scale PWR during prescribed transients in steam flow and vessel pressure. The LOCA transients used as input in the calculations are based on tabulated results of typical vendor and NRC evaluation model calculations for PWR's[28]. These results provide the required input for the present analysis in terms of time dependent values for downcomer steam flow rate, vessel pressure, flow rate and temperature of liquid entering the downcomer. Figure 38 describes three of the six steam flow transients for which calculations have been performed, representing different ramp time characteristics.

Time delay and plenum filling behavior were calculated according to our analysis. In addition, we have examined the most conservative case where we assumed that all wall heat flux is transferred as boiling component only, i.e., f = 0, and no condensation occurs in the system, i.e., $K^*_{cbp} = 0$. This case describes the hypothetical situation in which the largest possible amount of vapor is generated and no steam condensation occurs in the system, resulting in the maximum amount of countercurrent steam flow possible. Thus, the calculated time delays are the longest possible for a given set of conditions and are highly conservative.

As was done for the LOFT experiment (Section IV), calculations have been conducted for each case with two different assumptions concerning the film thickness. One set of calculations assumes that the film thickness (denoted by t_1) is given by the Nusselt equation. The other assumes that the liquid fills the annulus (film thickness is denoted by t_2), resulting in a more conservative set of results. The dependence of condensation on scale was taken in both cases as $\sim D^{*0.30}$, i.e., n = 0.30. This value for n is the same one used in the 1/5-scale comparisons. It is a conservative value since the condensation was found to depend on D^{*n} where n increases with scale. Indeed, if the n dependence on scale is extrapolated to a full scale, we find that n = 0.90.

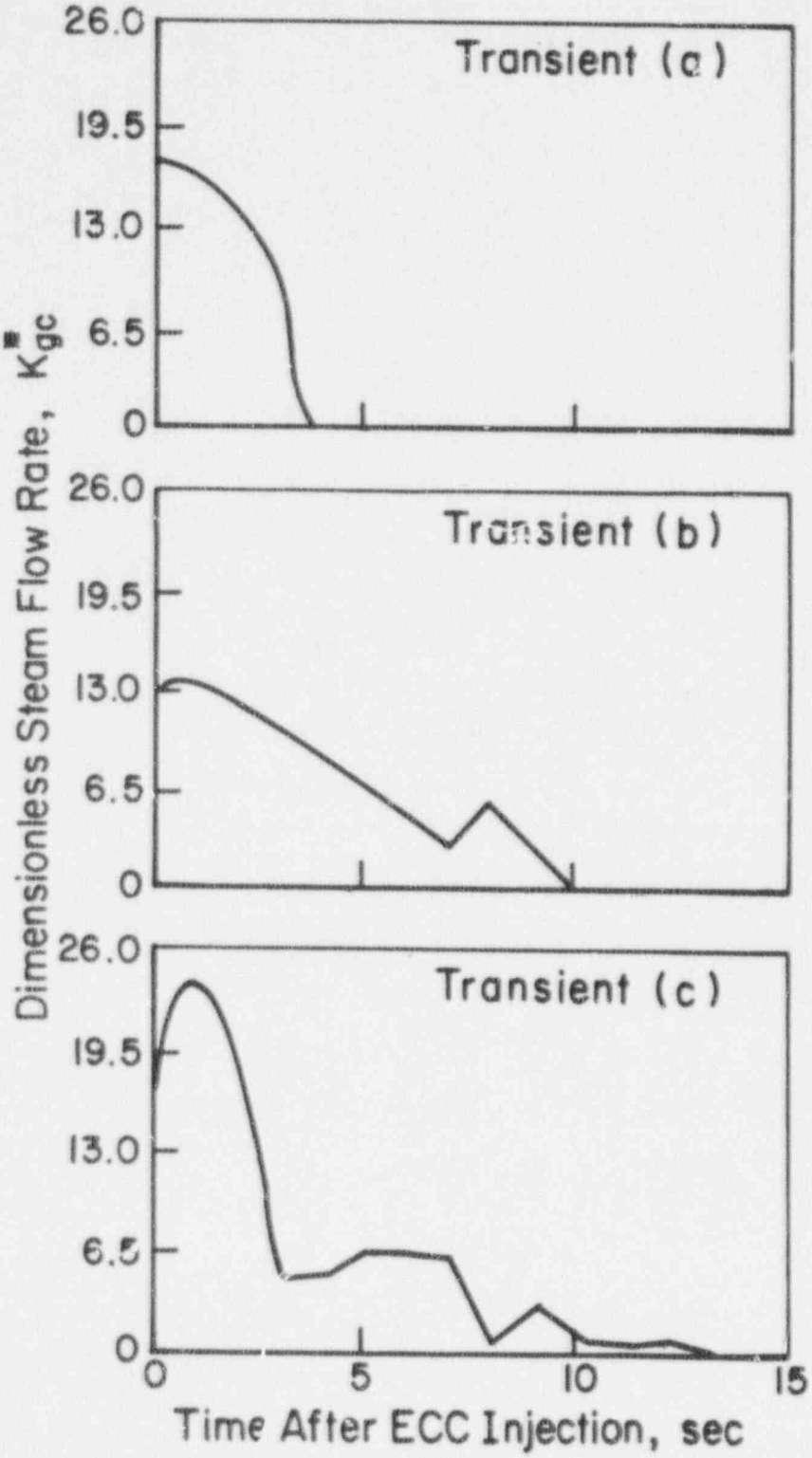

Figure 38. Dimensionless Steam Flow Rate Input for PWR Blowdown Transients (Reference 28)

Calculated time delays for the various transients and the two cases are given in Table 1. The delivery rates for all the transients were found to be essentially equal to the liquid injection rates. We have also calcuated the time delay according to a typical recommended licensing approach ("sequential method") in which:

Total Time Delay = Time At Which $W_{gc} = 0$

+ Gravity Fall Time From Cold Leg Height (1.1 sec)

+ Hot Wall Delay (2.2 sec)

As shown in Table 1, the time delay calaculated according to the licensing approach is always longer than that calculated by the present analysis, even for the most conservative assumptions.

There are several reasons to question the realism of the given LOCA transients themselves, as they were calculated with the assumptions of thermodynamic equilibrium and the decoupling of the core steam flow from major interaction with ECC flow[27].

TABLE 1. CALCULATED TIME DELAY, t_d

Transient	Best Estimate		Conservative Case		Licensing
	t_1	t_2	t_1	t_2	
(a)	1.2	4.4	4.5	4.5	6.7
(b)	2.0	10.0	10.0	12.1	13.3
(c)	2.0	8.0	13.0	15.1	16.3

VI. CONCLUSIONS

(1) Air-water data in 1/15- and 2/15-scale models are scaled better with a K^* parameter than with the J^* parameter which scales very small geometric sizes.

(2) The condensation efficiency parameters, f and f_1, depend on the liquid and steam flow rates, among others, and are not constant along the penetration curve.

(3) Simultaneous effects of mass and momentum exchange are accounted for reasonably well by a modified flooding correlation for the liquid penetration behavior.

(4) The effect of steam condensation on the injected water increases with scale size, resulting in more ECC penetration for a given dimensionless steam flux.

(5) Additional tests in the 2/5-scale model continue to show that K^* is the proper scaling parameter, and that the condensation effect increases with scale.

(6) The mechanistic model includes improved modeling of hot wall effects. The partitioning of wall heat flux is treated in a more mechanistic manner, than previously done.

(7) The consistently good agreement obtained for data in three different scale models and in the LOFT facility suggests that condensation effects, hot wall effects, dependence on scale, subcooling, and pressure, are well modeled by the present analysis.

(8) Application of the mechanistic model to full scale shows that the current licensing models are conservative even when highly conservative assumptions are made in the model.

(9) It is recommended that the K^* scaling continue to be used in licensing calculations with an allowance for increasing condensation effects.

REFERENCES

(1) Cudnik, R. A., et al, "Topical Report on Baseline Plenum Filling Behavior in a 2/15-Scale Model of a Four-Loop Pressurized Water Reactor", NUREG/CR-0069, BMI-1997 (April, 1978). Available from National Technical Information Service (NTIS), Springfield, Virginia 22161.

(2) Crowley, C. J., Block, J. A., and Cary, C. N., "Downcomer Effects in a 1/15-Scale PWR Geometry--Experimental Data Report", NUREG-0281, Creare TN-252 (February, 1977). Available from National Technical Information Service (NTIS), Springfield, Virginia 22161.

(3) Block, J. A., et al, "Analysis of ECC Delivery", Topical Report, Creare TN-231 (April, 1976). Available from National Technical Information Service (NTIS), Springfield, Virginia 22161.

(4) Carbiener, W. A., et al, "Steam-Water Mixing and System Hydrodynamics Program, Task 4", Quarterly Progress Report, October-December, 1977, NUREG/CR-0034, BMI-1993 (March, 1978). Available from National Technical Information Service (NTIS), Springfield, Virginia 22161.

(5) Beckner, W. D., Reyes, J. N., Jr., and Anderson, R., "Analysis of ECC Bypass Data", NUREG-0573, USNRC (July, 1979). Available from National Technical Information Service (NTIS), Springfield, Virginia 22161.*

(6) Alb, G. P., and Chambré, P. L., "Correlations for the Penetration of ECC Water in a Model of a PWR Downcomer Annulus", Nucl. Eng. and Design, 53, p. 237 (1979).

(7) Segev, A., and Collier, R. P., "A Mechanistic Model for Countercurrent Steam-Water Flow", J. of Heat Transfer, 102, p. 668 (1980).

(8) Segev, A., and Collier, R. P., "Topical Report on Development of a Mechanistic Model for ECC Penetration in a PWR Downcomer", NUREG/CR-1426, BMI-2051 (April, 1980). Available from National Technical Information Service (NTIS), Springfield, Virginia 22161.*

(9) Dworak, J. A., Segev, A., and Collier, R. P., "Scaling Air-Water Flooding in PWR Geometries", Trans. Amer. Nucl. Soc., 33, p. 973 (1979).

(10) Pushkina, O. L., and Sorokin, Y. L., "Breakdown of Liquid Film Motion in Vertical Tubes", Heat Transfer - Soviet Research, 1, No. 5, p. 55 (1969).

REFERENCES
(Continued)

(11) Wallis, G. B., "Flooding Velocities for Air and Water in Vertical Tubes", AEEW-R123, UKAEA (1961).

(12) Richter, H. J., and Wallis, G. B., "ECC Bypass Scaling", NUREG/CR-0850, USNRC (1979). Available from National Technical Information Service (NTIS), Springfield, Virginia 22161.*

(13) Rothe, P. H., and Crowley, C. J., "Scaling of Pressure and Subcooling for Countercurrent Flow", Quarterly Progress Report, April - June 1978, NUREG/CR-0464, Creare TN-285 (October, 1978). Available from National Technical Information Service (NTIS), Springfield, Virginia 22161.

(14) Segev, A., et al, "Countercurrent Steam Condensation and Its Application to ECC Penetration", Experimental and Analytical Modeling of LWR Safety Experiments, L. E. Hochreiter and G. L. Sozzi, ed., p. 101, ASME, New York (1980).

(15) Crowley, C. J., Sam, R. G., and Rothe, P. H., "1/5-Scale CCF Data Presentation and Discussion", Creare Technical Memorandum TM-741, January 1981.

(16) Saha, P., and Zuber, N., "Point of Net Vapor Generation and Vapor Void Fraction in Subcooled Boiling", Paper No. B4.7, in Proc. Fifth Int. Heat Trans. Conf., Tokyo, Vol. IV (1974).

(17) Segev, A., et al, "Steam-Water Mixing and System Hydrodynamics Program, Task 4", Quarterly Progress Report, January - March, 1980, NUREG/CR-1742, BMI-2065 (September, 1980). Available from National Technical Information Service (NTIS), Springfield, Virginia 22161.*

(18) Segev, A., Collier, R. P., and Flanigan, L. J., "Experimental Study of Hot Wall Effects on Liquid Flow", Trans. Amer. Nucl. Soc, 34, p. 468 (1980).

(19) Segev, A., Flanigan, L. J., and Collier, R. P., "Steam-Water Mixing and System Hydrodynamics Program,Task 4", April - June, 1980, NUREG/CR-1743, BMI-2067 (September, 1980). Available from National Technical Information Service (NTIS), Springfield, Virginia 22161.*

(20) Crowley, C. J., and Rothe, P. H., "Analysis of Superheated Wall Effects During Refill at Small Scale", NUREG/CR-0599, Creare TN-287 (1979). Available from National Technical Information Service (NTIS), Springfield, Virginia 22161.*

REFERENCES
(Continued)

(21) Segev, A., and Collier, R. P., "Steam-Water Mixing and System Hydrodynamics Program, Task 4", July - September, 1980, NUREG/CR-1822, BMI-2069 (November, 1980). Available from National Technical Information Service (NTIS), Springfield, Virginia 22161.*

(22) Batt, D. L., "Experimental Data Report of LOFT non-Nuclear Test L1-4", TREE-NUREG-1084, INEL (july, 1977).

(23) Robinson, H. C., "LOFT Systems and Test Description (Loss-of-Coolant Experiments Using a Core Simulator)", TREE-NUREG-1019, INEL (November, 1976).

(24) Grush, W. H., and Holmstron, H.L.O., "Post Test RELAP4 Analysis of LOFT Experiment L1-4", TREE-NUREG-1183, INEL (November 1977).

(25) Batt, D. L., "Downcomer Fluid Phenomena in LOFT Non-Nuclear LOCEs", NUREG/CR-0268, TREE-1139, INEL (August, 1978).

(26) Pyun, J. J., and Williams, K. A., "TRAC Analysis of Loss-of-Fluid Test Non-Nuclear Test L1-4", Nuclear Tech., 46, No. 3, p. 411 (1979).

(27) Crowley, C. J., et al, "Technical Summary Attachment to ECC Bypass RIL, Volume II: Technical Appendices", NUREG/CR-0885, 2; Creare TN-296, 2, July 1979. Available from National Technical Information Service (NTIS), Springfield, Virginia 22161.

(28) Cudnik, R. A., Letter to A. W. Serkiz, NRC, February 11, 1975.

*Also available for purchase from the NRC/GPO Sales Program, U.S. Nuclear Regulatory Commission, Washington, DC 20555.

NOMENCLATURE

A	Annulus cross section
C	Parameter
C_a	Average circumference
C_p	Specific heat of liquid
D^*	Bond number
f, f_l	Parameters
g	Gravitational acceleration
h_{fg}	Heat of vaporization
J_x^*	Dimensionless volumetric flux of phase x
j_x	Superficial velocity of phase x
k	Thermal conductivity
K_x^*	Dimensionless volumetric flux of phase x
K_{cbp}^*	Dimensionless volumetric flux of steam condensation on bypassed liquid
K_{gb}^*	Dimensionless volumetric flux of core steam at complete bypass point
K_{gc}^*	Dimensionless volumetric flux of core steam
$K_{\ell p}^*$	Dimensionless volumetric flux of penetrating liquid
L	Length of core barrel
ℓ	Distance
m	Parameter
n	Parameter

P, P_v, P_{Lp}	Pressure in lower plenum
P_h	Heated perimeter
Q	Heat transfer rate
Q^*	Dimensionless heat transfer rate
q	Heat flux
Re, $\overline{Re}$	Reynolds number
S	Gap size
T	Temperature
T_s	Saturation temperature
t, t_1, t_2	Film thickness
t	Time
t_d	Penetration time delay
V	Volume of liquid in lower plenum
V_o	Volume of lower plenum
W	Mass flow rate
z	Distance

GREEK

α	Thermal diffusivity
λ	Parameter
μ	Viscosity
ρ	Density
σ	Surface tension

SUBSCRIPTS

g	Vapor
i	Film inlet
in	Inlet of cold leg
ℓ	Liquid
o	Point of net vaporization
tm	Total net mass exchange
w	Wall

NRC FORM 335 (7-77) U.S. NUCLEAR REGULATORY COMMISSION

BIBLIOGRAPHIC DATA SHEET

1. REPORT NUMBER (Assigned by DDC)
NUREG/CR-2030
BMI-2077

4. TITLE AND SUBTITLE (Add Volume No., if appropriate)
Application of Battelle's Mechanistic Model to Lower Plenum Refill

2. (Leave blank)

3. RECIPIENT'S ACCESSION NO.

7. AUTHOR(S)
Aryeh Segev and Robert P. Collier

5. DATE REPORT COMPLETED
MONTH February YEAR 1981

9. PERFORMING ORGANIZATION NAME AND MAILING ADDRESS (Include Zip Code)
Battelle Columbus Laboratories
505 King Avenue
Columbus, Ohio 43201

DATE REPORT ISSUED
MONTH March YEAR 1981

6. (Leave blank)

8. (Leave blank)

12. SPONSORING ORGANIZATION NAME AND MAILING ADDRESS (Include Zip Code)
Division of Reactor Safety Research
Office of Nuclear Regulatory Research
U.S. Nuclear Regulatory Commission
Washington, DC 20555

10. PROJECT/TASK/WORK UNIT NO.

11. CONTRACT NO.
FIN No. A4048

13. TYPE OF REPORT
Topical Report

PERIOD COVERED (Inclusive dates)

15. SUPPLEMENTARY NOTES

14. (Leave blank)

16. ABSTRACT (200 words or less)

A mechanistic model has been developed to described the refill process of ECC during a postulated LOCA. The model analyzes a one-dimensional liquid film draining down a heated wall, in the presence of countercurrent steam flow. The effects of nonequilibrium void generation and steam condensation were investigated. These effects were incorporated into a momentum transfer correlation which was developed from air-water data in 1/15- and 2/15-scale models of PWR, with standard and distorted geometries. This correlation is based on the Kutateladze parameter and indicates that the overall momentum transfer between the phases does not depend on scale for geometrically similar models. Theoretical predictions were compared with results from steady-steam flow tests in 1/15, 2/15- and 1/5-scale models with adiabatic walls, hot wall tests with steady and ramped steam flows, and with test L1-4 conducted in the LOFT facility. The comparisons exhibit fairly good agreement. When applied to a full scale PWR, the analysis predicts that ECC penetration would occur at a time shorter than the recommended licensing time delay, even when highly conservative assumptions are made.

17. KEY WORDS AND DOCUMENT ANALYSIS

17a. DESCRIPTORS

ECC Bypass
Scaling
Condensation
Analysis Experiments

17b. IDENTIFIERS/OPEN-ENDED TERMS

18. AVAILABILITY STATEMENT
Unlimited

19. SECURITY CLASS (This report)
Unclassified

21. NO. OF PAGES

20. SECURITY CLASS (This page)

22. PRICE
$

*U.S. GOVERNMENT PRINTING OFFICE: 1981 341-742/788 1-3